

000  
001  
002  
003 

# DO MLLMs REALLY UNDERSTAND THE CHARTS?

  
004  
005  
006  
007  
008009 **Anonymous authors**  
010  
011  
012  
013  
014  
015  
016  
017  
018  
019  
020  
021  
022  
023  
024  
025  
026  
027  
028  
029  
030  
031  
032  
033  
034  
035  
036  
037  
038  
039  
040  
041  
042  
043  
044  
045  
046  
047  
048  
049  
050  
051  
052  
053009 Paper under double-blind review  
010  
011  
012  
013  
014  
015  
016  
017  
018  
019  
020  
021  
022  
023  
024  
025  
026  
027  
028  
029  
030  
031  
032  
033  
034  
035  
036  
037  
038  
039  
040  
041  
042  
043  
044  
045  
046  
047  
048  
049  
050  
051  
052  
053

## ABSTRACT

Although Multimodal Large Language Models (MLLMs) have demonstrated increasingly impressive performance in chart understanding, most of them exhibit alarming hallucinations and significant performance degradation when handling non-annotated charts<sup>1</sup>. We argue that current MLLMs rely largely on visual *recognition* rather than visual *reasoning* to interpret the charts, and visual estimation of numerical values is one of the most fundamental capabilities in chart understanding that require complex visual reasoning. To prove this, we introduce ChartVR-Bench, a benchmark meticulously designed to isolate and evaluate visual reasoning ability in chart understanding. Furthermore, we propose ChartVR-3B/7B trained with a novel Visual Reasoning Reinforcement Finetuning (VR-RFT) strategy to strengthen genuine chart visual reasoning abilities. Extensive experiments show that ChartVR achieves superior performance on ChartVRBench, outperforming even powerful proprietary models. Moreover, the visual reasoning skills cultivated by the proposed VR-RFT demonstrate strong generalization, leading to significant performance gains across a diverse suite of public chart understanding benchmarks. The code and dataset will be publicly available upon publication.

## 1 INTRODUCTION

Multimodal Large Language Models (MLLMs) (Bai et al., 2025; Comanici et al., 2025; OpenAI et al., 2024a; Lu et al., 2024) now play a pivotal role in the field of Artificial Intelligence, particularly for understanding complex visual data. These models have demonstrated a remarkable ability to process charts, analyze their content, provide insightful explanations, and achieve competitive performance against existing chart benchmarks (Wang et al., 2024; Masry et al., 2022; Xu et al., 2024b; Masry et al., 2025a; Xia et al., 2025).

Estimating numerical values from charts is a fundamental capability in chart understanding that involves interpreting visual representations to extract or approximate the underlying numbers. The core principle is to understand the mapping between the visual elements (e.g., the position, length, or angle of a mark) on the chart and the data scale it represents. However, when specific numerical annotations are missing from the chart, the propensity of MLLMs to hallucination increases dramatically (Xu et al., 2024b), as exemplified in Figure 1. This leads us to a fundamental question: *Do MLLMs really understand the charts?*

This failure suggests that current MLLMs excel at recognizing about *textual content* within charts but struggle profoundly with reasoning from their underlying *visual geometry*. We argue that it stems from the fundamental reliance of MLLMs on textual *recognition* over genuine visual *reasoning*. To systematically diagnose this core ability, we introduce the Chart Visual Reasoning Benchmark (*ChartVRBench*), which is meticulously designed to isolate numerical value estimation on non-annotated charts, forcing models to move beyond textual recognition. The evaluation reveals that not only open-source MLLMs (Bai et al., 2025; Zhu et al., 2025; Lu et al., 2024) face performance degradation, but even powerful close-source MLLMs, such as GPT-4o (OpenAI et al., 2024a) and Gemini-2.5-Flash (Comanici et al., 2025), also struggle significantly with ChartVRBench.

Moreover, inspired by the success of Reinforcement Learning (RL) in enhancing textual reasoning for mathematics and coding (DeepSeek-AI et al., 2025; OpenAI et al., 2024b; Tan et al., 2025; Huang et al., 2025), we propose ChartVR, a series of MLLMs forged with a novel Visual Reasoning

<sup>1</sup>The non-annotated charts are those that require viewers to estimate values using the vertical/horizontal axis scale.

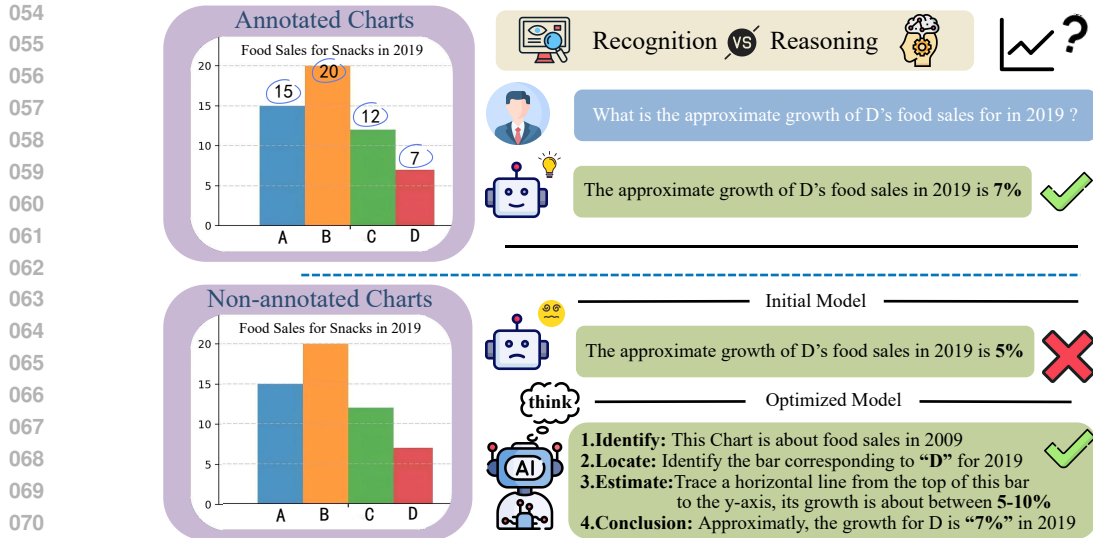


Figure 1: Illustration of the visual reasoning deficit in MLLMs when processing non-annotated charts. A standard model, limited by its underdeveloped visual reasoning capacity, often resorts to guessing and fails. In contrast, our ChartVR executes a deliberate, human-like reasoning chain—identifying the target, locating data based on visual scales, and forming a conclusion—to successfully estimate the value.

Reinforcement Finetuning (VR-RFT) strategy to strengthen genuine chart visual reasoning abilities. The first stage, Visual Reasoning Activation, uses a Chain-of-Thought Supervised Finetuning (CoT-SFT) (Liu et al., 2023) to compel the model to externalize a step-by-step analysis of the chart’s visual components. This forces the model to learn an explicit protocol for geometric interpretation, such as locating axes and grounding queries to graphical marks, thereby forming the structural foundation of its visual reasoning capability. Building on this, the second stage, Visual Reasoning Generalization, employs Group Relative Policy Optimization (GRPO) (Shao et al., 2024) to further refine this process. By training on a curated dataset of ambiguous samples where the initial model’s judgment is inconsistent, we force it to make finer perceptual discriminations. This training process is guided by a novel continuous accuracy reward function with a quadratic formulation, providing a dense signal directly proportional to the accuracy of the visual estimation. In summary, these stages steer ChartVR to a robust, generalizable visual reasoning capability for charts.

The extensive experiments demonstrate that ChartVR achieves superior performance on ChartVR-Bench, even comparable to powerful proprietary models like Gemini-2.5-Flash (Comanici et al., 2025). More importantly, we demonstrate that the foundational skill cultivated by our method is highly generalizable. ChartVR exhibits significant performance gains across a diverse suite of public, multi-task chart understanding benchmarks (Wang et al., 2024; Xu et al., 2024b; Masry et al., 2025a), proving the effectiveness of our approach in building more rational and reliable MLLMs for chart comprehension.

The main contributions of this work are summarized as follows:

- We introduce *ChartVRBench*, a distinctive benchmark designed to isolate and evaluate genuine visual reasoning capability in chart understanding. It overcomes the limitations of prior work by focusing exclusively on numerical estimation tasks, thus disentangling reasoning from text recognition.
- We propose *ChartVR*, a series of MLLMs with significantly enhanced visual reasoning capabilities for chart understanding. It achieves excellent performance on our challenging ChartVR-Bench, compared with chart-specific and general MLLMs, even surpassing powerful proprietary models like Gemini-2.5-Flash.
- We demonstrate that the visual reasoning ability cultivated by our method is foundational and highly generalizable. *ChartVR* is not confined to the specific numerical estimation task, but

108 achieves substantial performance gains across a diverse suite of public, multi-task chart under-  
 109 standing benchmarks.  
 110

111 **2 RELATED WORK**

112 **2.1 CHART UNDERSTANDING BENCHMARKS**

113 A suite of benchmarks has been developed to evaluate the chart comprehension capabilities of  
 114 MLLMs. Early benchmarks, such as ChartQA (Masry et al., 2022) and PlotQA (Methani et al.,  
 115 2020), primarily focused on descriptive tasks. More recently, benchmarks like CharXiv (Wang et al.,  
 116 2024), ChartQAPro (Masry et al., 2025a), and ChartMuseum (Tang et al., 2025a) have raised the bar  
 117 by incorporating complex questions and diverse, real-world charts. While these works encompass  
 118 a wide range of tasks, they often conflate general reasoning with the core challenge of visual inter-  
 119 pretation. The most related work to ours is ChartBench (Xu et al., 2024b); while it also focuses on  
 120 non-annotated charts, it is composed of mostly synthetic data with limited visual diversity. Similarly,  
 121 recent work by Mukhopadhyay et al. (2024) revealed critical flaws in the consistency and robustness  
 122 of MLLMs but stopped short of attributing these shortcomings to a fundamental deficit in visual  
 123 reasoning. We argue this deficit—the core skill of visual reasoning in a chart’s geometry, such as  
 124 numerical value estimation—remains largely untested. Our ChartVRBench is specifically designed  
 125 to isolate and evaluate this crucial visual reasoning capability.  
 126

127 **2.2 CHART UNDERSTANDING WITH MLLMs**

128 Many general-purpose MLLMs, such as gpt-4o (OpenAI et al., 2024a), Gemini-2.5 Series (Co-  
 129 manici et al., 2025), and Qwen (Bai et al., 2025), are increasingly applied to chart understanding  
 130 tasks. In parallel, the development of specialized Chart MLLMs has been rapid, with many models  
 131 like ChartLlama (Han et al., 2023) and ChartGemma (Masry et al., 2025c). However, their devel-  
 132 opment has largely depended on SFT, a paradigm that, as we argue, tends to cultivate superficial  
 133 recognition at the expense of genuine reasoning. Recognizing this, a recent wave of models (Chen  
 134 et al., 2025; Masry et al., 2025b), have incorporated RL to enhance complex, multi-step reason-  
 135 ing. While these RL-based approaches represent a significant step forward, their training objectives  
 136 often prioritize the final accuracy of text-heavy queries, which can leave the foundational skill of  
 137 visual grounding underdeveloped. In contrast, our ChartVR is specifically designed to address this  
 138 fundamental layer. Its RFT framework is meticulously crafted to cultivate the core ability to reason  
 139 directly from visual geometry, aiming to develop a genuine visual reasoning capability rather than  
 140 optimizing the textual reasoning that typically follows.  
 141

142 **2.3 REASONING IN CHART UNDERSTANDING**

143 Reinforcement Learning (RL) has been successfully employed to enhance the reasoning abilities  
 144 of Large Language Models (LLMs), allowing them to move beyond the static data distributions of  
 145 SFT (Ouyang et al., 2022). By learning from reward feedback, models have shown significant im-  
 146 provements in complex domains like mathematics and coding (DeepSeek-AI et al., 2025; Shao et al.,  
 147 2024). Inspired by this success, several works have begun to apply similar RL-based paradigms to  
 148 MLLMs (Feng et al., 2025; Tan et al., 2025; Huang et al., 2025), activating their visual reasoning  
 149 on tasks like visual counting and spatial transformation. Building on these advancements, our work  
 150 adapts this powerful paradigm to the specialized domain of chart understanding.  
 151

152 **3 CHARTVRBENCH**

153 We introduce Chart Visual Reasoning Benchmark (ChartVRBench), a comprehensive, multi-  
 154 domain, and reasoning-centric benchmark designed to rigorously assess the visual interpretation  
 155 capabilities of MLLMs on charts that lack explicit numerical annotations. Engineered to move be-  
 156 yond simple OCR-dependent tasks, the benchmark comprises a total of 2,453 question-answer pairs.  
 157 It features a majority (2,101 pairs) of synthetically generated charts to ensure controlled complex-  
 158 ity and a significant portion (352 pairs) sourced from real-world examples to guarantee practical  
 159 relevance.  
 160

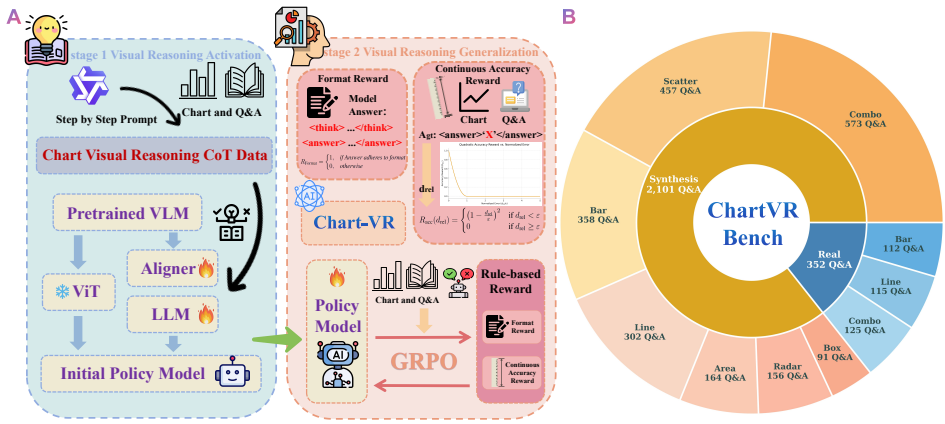


Figure 2: The training paradigm of ChartVR and the data distribution of ChartVRBench. A: ChartVR leverages a two-stage RFT strategy. Stage 1 activates the model’s reasoning abilities via SFT on CoT data, while Stage 2 uses GRPO with a multi-component reward system to reinforce correct chart understanding. B: The composition of ChartVRBench, detailing the distribution of seven chart types across both synthetic and real data sources.

Table 1: Comparison between ChartVRBench and existing representative chart QA benchmarks. Symbols: ✓ Fully Supported / High Quality; △ Partially Supported / Mixed; × Not Supported / Low Quality.

Feature	EvoChart Huang et al. (2024)	ChartBench Xu et al. (2024b)	CharXiv Wang et al. (2024)	ChartQAPro Masry et al. (2025a)	ChartMuseum Tang et al. (2025a)	Ours
Real-World Charts	✓	✗	✓	✓	✓	✓
Broad Topic Coverage	✗	✗	△	△	△	✓
Non-Annotated Charts	✗	✓	✗	✗	✗	✓
Isolates Visual Reasoning	✗	△	✗	✗	✓	✓

The benchmark provides extensive coverage across seven primary chart types, including bar, line, scatter, and combo charts, with a detailed breakdown of the data distribution shown in Figure 2. This structural diversity is complemented by thematic breadth, with data spanning 38 distinct topics, including finance, healthcare, and technology. This dual emphasis on structural and thematic variety ensures a rigorous evaluation, mitigating the risk of models overfitting to specific chart formats or familiar domains.

While existing benchmarks have significantly advanced the field, they predominantly focus on general high-level Question Answering (QA), where visual reasoning is often conflated with textual extraction (OCR) and logical reasoning. ChartVRBench fills a critical gap by strictly isolating the visual reasoning capability of numerical value estimation on non-annotated charts, preventing models from relying on text recognition shortcuts. To clearly demonstrate how our benchmark compares to contemporary works, we present a feature-wise comparison in Table 1.

### 3.1 DATA CURATION

**Synthetic Chart Generation.** Our synthetic chart generation process is partially adapted from the Code-as-Intermediary Translation (CIT) methodology proposed by He et al. (2024), where executable plotting code serves as the ground truth for each chart. The process begins with a curated set of seed scripts, which are then programmatically diversified using Self-Instruct (Wang et al., 2023) and Evol-Instruct (Xu et al., 2024a) techniques to generate a vast library of visually complex charts. A critical constraint is the deliberate omission of numerical labels on data points, ensuring that every chart necessitates visual estimation. To maximize yield, a self-repair mechanism leverages an LLM to debug and correct any code that fails during execution. Following an automated visual fidelity check by a MLLM, the entire collection of synthesized data underwent a final, rigorous human review. This manual verification step served to confirm the high quality of the chart images and the accuracy of their corresponding question-answer pairs. This code-centric approach, combined

216 with multiple stages of validation, provides an unimpeachable ground truth, allowing us to generate  
 217 verifiably correct Q&A pairs.  
 218

219 **Real Chart Collection.** To anchor our benchmark in real-world applications, we sourced charts  
 220 from reputable data repositories such as Statista and Our World in Data. Each chart was manually  
 221 vetted by human annotators to meet strict criteria: high visual quality, data integrity, and a complete  
 222 absence of explicit numerical annotations. Following selection, an MLLM was used to generate  
 223 candidate question-answer pairs for each chart. Every MLLM-generated pair then underwent a final  
 224 round of human verification and refinement to guarantee the accuracy and relevance of both the  
 225 question and its ground-truth answer.

226 **3.2 EVALUATION PROTOCOL**

227 Standard exact-match accuracy is ill-suited for value estimation from non-annotated charts, as it  
 228 fails to account for the slight perceptual ambiguity inherent in the task, even for human observers.  
 229 To address this, we employ a relaxed accuracy metric, which judges a prediction correct if its relative  
 230 error from the ground-truth value falls within a tolerance threshold, denoted as  $\tau$ . To align  
 231 this threshold with human performance, we conducted an empirical study and found that human  
 232 estimations consistently fall within a 2% error margin. Accordingly, we empirically set  $\tau = 0.02$ .  
 233

234 Formally, a model’s predicted value,  $A_{pred}$ , is deemed correct if and only if it satisfies the following  
 235 condition relative to the ground truth,  $A_{gt}$ :

$$A_{pred} \in [(1 - \tau) \times A_{gt}, (1 + \tau) \times A_{gt}]$$

236 This protocol ensures that our evaluation is both rigorous and fairly aligned with human-level interpretive  
 237 capabilities, rewarding models for precise visual reasoning rather than penalizing them for  
 238 minor, human-like estimation variance.

242 **4 CHARTVR**

243 We propose ChartVR, a series of MLLMs designed to perform visual reasoning for better visual  
 244 understanding on non-annotated charts. We formally define this task as follows: given a chart  
 245 image  $I$ , and a corresponding textual question  $Q$ , the goal is to derive a numerical answer  $A$  with a  
 246 reasoning procedure  $R$ . This process can be represented as a mapping function  $\mathcal{F}$ :

$$\mathcal{F} : (I, Q) \rightarrow (R, A)$$

247 where  $I$  is the chart image,  $Q$  is the question in text,  $R$  is the step-wise reasoning procedure in text,  
 248 and  $A \in \mathbb{R}$  is the numerical answer. The fundamental challenge lies in interpreting non-annotated  
 249 charts, which requires the model to reason about geometric structures (e.g., axes, scales, positions)  
 250 to infer values, rather than simply extracting them via text recognition.

251 To address this challenge, we propose a novel two-stage Reinforcement Finetuning (RFT) frame-  
 252 work. This approach is designed to first instill a robust, human-like reasoning framework and then  
 253 meticulously refine the model’s numerical precision. As illustrated in Figure 2, the RFT pipeline  
 254 consists of two sequential stages: (1) Visual Reasoning Activation, which uses supervised fine-  
 255 tuning to teach the model the structure of reasoning, followed by (2) Visual Reasoning Generaliza-  
 256 tion, which uses reinforcement learning to improve the accuracy and generalizability.

261 **4.1 STAGE 1: VISUAL REASONING ACTIVATION**

262 The initial stage of our pipeline aims to establish a foundational reasoning paradigm. Instead of  
 263 having the model directly guess an answer, we teach it to adopt a structured, step-by-step thought  
 264 process that mirrors human analysis. To achieve this, we fine-tune our base model on a high-quality  
 265 dataset of 43k samples generated by distilling detailed Chain-of-Thought (CoT) processes from an  
 266 advanced MLLM (see Appendix B.1 for details). This CoT-SFT process systematically teaches the  
 267 model to move beyond direct answer prediction and instead adopt a structured analytical approach:  
 268 first identifying and utilizing critical chart components—such as axes, scales, and legends—and then  
 269 using them to derive a final answer.

270 Formally, we employ SFT on this dataset. Each data instance is a tuple  $(x, q, r, a)$ , where  $x$  is the  
 271 chart image,  $q$  is the question,  $r$  is the intermediate reasoning chain, and  $a$  is the final answer. The  
 272 training objective is to minimize the negative log-likelihood of the model generating the complete  
 273 sequence  $y$  (the concatenation of  $r$  and  $a$ ) given the image  $x$  and question  $q$ :

$$275 \quad \mathcal{L}_{\text{SFT}} = -\mathbb{E}_{(x, q, r, a) \sim \mathcal{D}} \sum_{t=1}^{|y|} \log \pi_{\theta}(y_t | x, q, y_{<t}) \quad (1)$$

278 where  $\mathcal{D}$  is our CoT dataset and  $\pi_{\theta}$  is the policy of the model with parameters  $\theta$ . The resulting  
 279 fine-tuned model, denoted as  $\pi_{\text{SFT}}$ , learns a robust template for visual reasoning and serves as the  
 280 starting point for the next stage.

## 282 4.2 STAGE 2: VISUAL REASONING GENERALIZATION

284 Building on the visual reasoning foundation from Stage 1, the second stage focuses on enhancing the  
 285 model’s precision and reliability for the numerical estimation task. For this, we use a smaller, high-  
 286 signal dataset of 3.4k samples curated to target the model’s specific weaknesses. These samples are  
 287 identified by selecting problems where the SFT-tuned model exhibits “stochastic correctness”—that  
 288 is, problems it can solve but not consistently (see Appendix B.3 for details). By training on these  
 289 borderline cases with higher-resolution images, we force the model to refine its visual interpretation  
 290 skills.

291 We employ GRPO (Shao et al., 2024), an efficient and scalable reinforcement learning algorithm,  
 292 to fine-tune the policy model  $\pi_{\text{SFT}}$ . Unlike traditional algorithms like PPO (Schulman et al., 2017),  
 293 GRPO forgoes a computationally expensive value network and instead calculates relative advantages  
 294 by comparing rewards within a group of sampled responses. For each input  $(x, q)$ , we sample a  
 295 group of  $G$  candidate answers  $\{a_1, a_2, \dots, a_G\}$  from the current policy  $\pi_{\beta}$ . Each answer  $a_i$  receives  
 296 a reward  $R(a_i)$ , and these rewards are used to compute a normalized relative advantage  $A_i$  for each  
 297 sample:

$$298 \quad A_i = \frac{r_i - \text{mean}\{r_1, \dots, r_G\}}{\text{std}\{r_1, \dots, r_G\}} \quad (2)$$

300 The policy is then updated to increase the probability of actions with positive advantages, while a  
 301 KL-divergence penalty against the reference model  $\pi_{\text{SFT}}$  ensures stable training.

## 302 4.3 REWARD FUNCTION DESIGN

304 The effectiveness of our RL stage hinges on a well-designed reward function. Our function  $R(a_i)$  is  
 305 a composite of two components, targeting both response structure and numerical accuracy:

$$307 \quad R(a_i) = R_{\text{format}}(a_i) + R_{\text{acc}}(a_i) \quad (3)$$

309 **Format Reward.** To encourage interpretable and well-structured outputs, we provide a binary  
 310 format reward,  $R_{\text{format}}$ . The model receives a reward of 1 if its response strictly adheres to our  
 311 predefined template, where reasoning is enclosed in `<think></think>` tags and final answer in  
 312 `<answer></answer>` tags, and 0 otherwise.

314 **Continuous Accuracy Reward.** To overcome the sparse signal from a simple correct/incorrect  
 315 binary reward, we introduce a continuous accuracy reward,  $R_{\text{acc}}$ . This reward provides a fine-grained  
 316 signal that recognizes “nearly correct” answers. For a predicted answer  $A_{\text{pred}}$  and a non-zero ground  
 317 truth  $A_{\text{gt}}$ , we first calculate the relative error:

$$318 \quad d_{\text{rel}} = \frac{|A_{\text{pred}} - A_{\text{gt}}|}{|A_{\text{gt}}|} \quad (4)$$

321 Then, we define the reward using a piecewise quadratic function that smoothly decays from 1 to 0:

$$322 \quad R_{\text{acc}}(d_{\text{rel}}) = \begin{cases} \left(1 - \frac{d_{\text{rel}}}{\tau}\right)^2 & \text{if } d_{\text{rel}} < \tau \\ 0 & \text{if } d_{\text{rel}} \geq \tau \end{cases} \quad (5)$$

324 Table 2: Comparison of ChartVR with representative MLLMs on the proposed ChartVRBench. The  
 325 best and second-best scores in each column are highlighted using bold and underline formatting,  
 326 respectively.

328 <b>Methods</b>	329 <b>Synthetic Charts</b>							330 <b>Real Charts</b>			331 <b>Overall</b>
	332 Box	333 Area	334 Radar	335 Scatter	336 Bar	337 Line	338 Combo	339 Bar	340 Line	341 Combo	
330 <b>Human Evaluation</b>	345 94.51	346 43.29	347 88.46	348 91.24	349 96.65	350 97.68	351 90.92	352 84.82	353 84.35	354 65.60	355 87.57
<i>Open-source Models</i>											
332 InternVL3-2B (Zhu et al., 2025)	333 25.27	334 8.54	335 9.62	336 25.16	337 51.68	338 43.05	339 34.55	340 43.75	341 34.78	342 32.00	343 32.98
333 Qwen2.5-vl-3B (Bai et al., 2025)	334 46.15	335 14.02	336 17.95	337 51.42	338 72.91	339 81.13	340 62.83	341 66.96	342 54.78	343 45.60	344 56.62
334 Ovis1.6-llama3.2-3B (Lu et al., 2024)	335 12.09	336 3.66	337 7.69	338 14.66	339 13.13	340 10.93	341 11.69	342 8.04	343 16.52	344 12.00	345 11.66
335 Gemma-3-4B (Team et al., 2025)	336 9.89	337 3.05	338 12.82	339 11.82	340 9.22	341 12.25	342 6.81	343 8.04	344 12.17	345 7.20	346 9.34
336 Qwen2.5-vl-7B (Bai et al., 2025)	337 70.33	338 21.34	339 19.23	340 61.93	341 73.74	342 85.43	343 68.41	344 49.11	345 56.52	346 48.00	347 61.39
337 InternVL3-8B (Zhu et al., 2025)	338 36.73	339 12.80	340 12.18	341 39.17	342 43.58	343 47.68	344 36.82	345 38.39	346 46.09	347 34.40	348 36.73
<i>Close-source Models</i>											
338 GPT-4o (OpenAI et al., 2024a)	339 28.57	340 12.20	341 11.54	342 25.61	343 21.23	344 27.15	345 18.15	346 13.39	347 26.96	348 18.40	349 20.87
339 Gemini-2.5-Flash (Comanici et al., 2025)	340 68.13	341 25.61	342 7.69	343 61.93	344 72.07	345 75.17	346 55.85	347 49.11	348 52.17	349 39.20	350 55.77
<i>Chart-Specific Models</i>											
340 ChartGemma-3B (Masry et al., 2025c)	341 10.99	342 10.98	343 7.05	344 21.44	345 42.74	346 32.78	347 24.43	348 37.50	349 42.61	350 28.80	351 26.74
341 TinyChart-3B (Zhang et al., 2024)	342 13.19	343 7.93	344 7.69	345 25.16	346 56.15	347 54.30	348 36.65	349 57.14	350 40.87	351 34.40	352 35.83
342 ChartInstruct-7B (Masry et al., 2024)	343 10.99	344 1.22	345 4.49	346 16.63	347 35.47	348 16.56	349 18.85	350 51.79	351 45.22	352 18.40	353 20.91
343 ChartVLM-7.3B (Xia et al., 2025)	344 9.89	345 10.37	346 7.69	347 10.28	348 70.39	349 45.36	350 32.81	351 50.00	352 54.78	353 35.20	354 33.63
344 ChartLlama-13B (Han et al., 2023)	345 10.99	346 1.83	347 5.77	348 5.25	349 3.35	350 4.30	351 4.01	352 8.04	353 9.57	354 7.20	355 5.01
345 Bespoke-MiniChart-7B (Tang et al., 2025b)	346 72.53	347 26.83	348 25.00	349 66.74	350 86.87	351 89.40	352 75.04	353 <b>69.64</b>	354 <b>62.61</b>	355 <b>45.60</b>	356 <b>68.16</b>
346 Chart-R1 (7B) (Chen et al., 2025)	347 <b>83.52</b>	348 26.22	349 <u>25.64</u>	350 <u>66.83</u>	351 85.47	352 82.45	353 68.94	354 <u>61.61</u>	355 <u>59.13</u>	356 44.80	357 65.72
347 <b>ChartVR-3B (Ours)</b>	348 63.74	349 24.39	350 19.87	351 57.33	352 82.68	353 87.75	354 69.46	355 58.93	356 57.39	357 45.60	358 62.74
348 <b>ChartVR-7B (Ours)</b>	349 <b>83.52</b>	350 <b>37.20</b>	351 <b>27.56</b>	352 <b>70.90</b>	353 <b>88.27</b>	354 <b>92.05</b>	355 <b>78.53</b>	356 <b>69.64</b>	357 <b>62.61</b>	358 <b>58.40</b>	359 <b>72.20</b>

348 We empirically set  $\tau = 0.02$  based on a human-calibrated tolerance threshold. For the specific  
 349 case where the ground truth  $A_{gt}$  is zero, because it is difficult to quantize the relative deviations, the  
 350 accuracy reward falls back to exact match, assigning a value of 1 when  $A_{gt} = A_{pred}$  and 0 otherwise.  
 351

352 We employ the quadratic formulation for two critical reasons. First, this design provides a clear,  
 353 bounded, and intuitive reward range. It yields a reward of 1 for a perfect answer ( $d_{rel} = 0$ ) and  
 354 smoothly decay to 0 as the relative error hits the 2% tolerance boundary. Second, the quadratic  
 355 shape creates a desirable non-linear decay. It has a gentle slope for subtle errors, granting sub-  
 356 stantial partial credit for close answers, while the penalty accelerates as the error approaches the  
 357 tolerance threshold. This behavior encourages the model to make fine-grained improvements when  
 358 it is already close to the correct answer, while strongly penalizing larger, unacceptable deviations.  
 359

## 360 5 EXPERIMENTS

### 361 5.1 EXPERIMENTAL SETUPS

362 **Implementation Details.** The implementation was built upon the ModelScope SWIFT frame-  
 363 work (Zhao et al., 2025). We initialize our ChartVR models using the open-source Qwen2.5-VL  
 364 series (Bai et al., 2025) as a foundation. For inference, all models and benchmarks follow their  
 365 provided settings where available, with results obtained from a single forward pass using a fixed  
 366 random seed of 42 to ensure reproducibility. Additional details are available in Appendix C.  
 367

368 **Main Evaluation on ChartVRBench.** Our primary evaluation is conducted on the proposed  
 369 ChartVRBench to assess genuine visual reasoning capabilities and establish the superiority of our  
 370 ChartVR model. On this benchmark, we compare our model against a comprehensive suite of base-  
 371 lines organized into three categories: open-source MLLMs, powerful close-source MLLMs and  
 372 prominent chart-specific models.

373 **Generalization Study on Public Benchmarks.** To evaluate the transferability of the skills learned  
 374 via our RFT framework, we conduct a generalization study. Specifically, we benchmark our  
 375 ChartVR model against the representative chart-specific models—ChartGemma (Team et al., 2025),  
 376 TinyChart (Zhang et al., 2024), ChartInstruct (Masry et al., 2024), ChartVLM (Xia et al., 2025),  
 377

378 Table 3: Performance of ChartVR compared to other chart-specific models on various public chart  
 379 understanding benchmarks. All results are reproduced by the authors. Qwen2.5-VL baselines are  
 380 listed below their corresponding ChartVR models with an arrow indicator. The best and second-best  
 381 scores in each column are highlighted using bold and underline formatting, respectively.

Models	ChartVRBench	CharXiv (R)	ChartBench	ChartQAPro
ChartGemma-3B (Masry et al., 2025c)	26.74	12.50	-	6.84
TinyChart-3B (Zhang et al., 2024)	35.83	8.30	-	13.25
ChartInstruct-7B (Masry et al., 2024)	20.91	8.80	-	4.88
ChartVLM-7.3B (Xia et al., 2025)	33.63	-	12.06	-
ChartLlama-13B (Han et al., 2023)	5.01	14.20	21.30	-
Bespoke-MiniChart-7B (Tang et al., 2025b)	<b>68.16</b>	41.40	<u>44.19</u>	34.74
Chart-R1 (7B) (Chen et al., 2025)	65.80	<b>50.00</b>	15.71	31.81
<b>ChartVR-3B (Ours)</b>	62.74	33.40	26.35	28.03
→ Qwen2.5-VL-3B (Bai et al., 2025)	56.62	30.60	21.30	24.51
<b>ChartVR-7B (Ours)</b>	<b>72.20</b>	<u>43.40</u>	<b>45.34</b>	<b>41.79</b>
→ Qwen2.5-VL-7B (Bai et al., 2025)	61.39	39.50	35.35	<u>37.10</u>

394  
 395 and ChartLlama (Han et al., 2023)—on a diverse set of public benchmarks. This suite includes the  
 396 real-world datasets CharXiv (Wang et al., 2024) and ChartQAPro (Masry et al., 2025a), as well as  
 397 the synthetic benchmark ChartBench (Xu et al., 2024b). This allows us to verify that our training  
 398 methodology imparts a foundational reasoning ability that generalizes effectively to a variety of  
 399 chart understanding tasks.  
 400

## 401 5.2 EXPERIMENTAL RESULTS

402  
 403 **Performance on ChartVRBench.** The results, presented in Table 2, underscore the significant  
 404 challenge that ChartVRBench poses to a wide range of MLLMs. The generally low scores across  
 405 all categories—including powerful proprietary models like GPT-4o (20.87%) and Gemini-2.5-Flash  
 406 (55.77%)—reveal a critical and widespread weakness in genuine visual reasoning. This difficulty  
 407 stems from our benchmark’s design, which forces models to infer values from graphical geometry  
 408 (e.g., axes and scales) rather than relying on OCR-based shortcuts common in other benchmarks.  
 409 The particularly low score of GPT-4o has been double-checked and manually validated, which pre-  
 410 cisely indicates that many MLLMs lack the genuine visual reasoning ability, as we argue.

411 Our proposed model, ChartVR, demonstrates a clear superiority in this demanding task. ChartVR-  
 412 7B achieves an overall score of 72.20%, outperforming all other models, including the best open-  
 413 source baseline, Qwen2.5-vl-7B (61.39%), and the strongest proprietary model, Gemini-2.5-Flash.  
 414 Notably, even our smaller ChartVR-3B model (62.74%) surpasses most other models, highlighting  
 415 the effectiveness of our training methodology. The performance is particularly strong on complex  
 416 chart types like Real Combo charts, where ChartVR-7B (58.40%) dramatically outperforms the  
 417 other models.

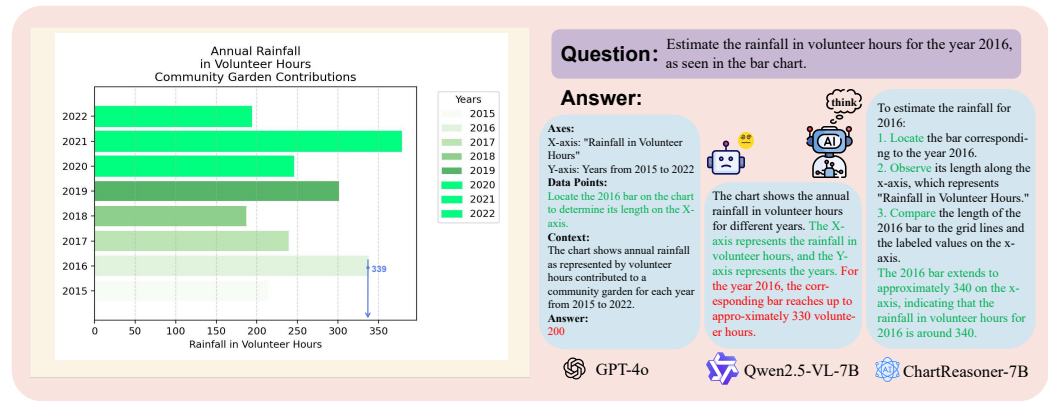
418  
 419 **Generalization on Public Benchmarks.** As detailed in Table 3, ChartVR-7B exhibits excep-  
 420 tional generalization, achieving competitive results across the board. Specifically, on the reasoning-  
 421 focused portion of CharXiv, our model achieves an improvement of 3.9% over the base model  
 422 Qwen2.5-VL-7B. This success stems from our model’s core visual reasoning capability, which con-  
 423 trasts with other chart-specific models that rely on SFT and often fail to develop a generalizable  
 424 reasoning capability.

## 425 5.3 ABLATION STUDY

426  
 427 **Effectiveness of the RFT Training Paradigm.** To systematically validate our training strate-  
 428 gies, we conducted an comparative study comparing three paradigms: CoT-SFT, GRPO applied  
 429 directly to the base model, and our full RFT framework. The results are summerized in Table 4. For  
 430 ChartVR-7B, the base model scores 61.39%. Using CoT data as a ‘Visual Reasoning Activation’  
 431 merely compels the model to adopt a visual reasoning pattern without imparting the underlying abil-  
 432 ity. Consequently, this mismatch leads to a performance degradation rather than an improvement.

432 Table 4: Ablation study of training strategies for ChartVR-3B and  
 433 ChartVR-7B models. The best and second-best scores are high-  
 434 lighted.

436 <b>Training Paradigm</b>	437 <b>ChartVR-3B</b>			438 <b>ChartVR-7B</b>			<b>Reward Component</b>	<b>Score</b>
	439 Synthetic	440 Real	441 Overall	439 Synthetic	440 Real	441 Overall		
439 Zero-Shot	<b>56.87</b>	<b>54.78</b>	56.52	<b>67.66</b>	51.16	61.39	Format	61.84
+Cot-SFT	36.55	34.86	40.77	55.45	45.74	54.06	Cont. Acc	67.88
+GRPO	56.59	<b>56.82</b>	<b>56.62</b>	66.44	<b>54.83</b>	64.78	Acc + Format	70.28
+RFT	<b>64.26</b>	53.69	<b>62.74</b>	<b>73.68</b>	<b>63.35</b>	<b>72.20</b>	<b>Cont. Acc + Format</b>	<b>72.20</b>



457 Figure 3: Qualitative analysis on ChartVRBench. GPT-4o and Qwen2.5-VL-7B exhibits hallucination in the answer and reasoning procedure, respectively. In contrast, our ChartVR-7B is able to 458 produce a coherent and correct step-by-step reasoning process, leading to an accurate answer.  
 459

460  
 461 In contrast, the full RFT framework, which synergistically combines SFT with RL, achieves the  
 462 most significant performance gain, reaching 72.20%. This demonstrates that our complete VR-RFT  
 463 framework genuinely enhances the model’s visual reasoning ability, leading to its consistent and  
 464 substantial outperformance over all other configurations.  
 465

466  
 467 **Impact of the Reward Function Design.** We conducted an ablation study to isolate the contribu-  
 468 tion of each component in our reward function, with results presented in Table 5. The findings  
 469 highlight a strong synergistic effect between enforcing a correct output structure and rewarding nu-  
 470 merical precision. A model trained with only the Format reward achieves a score of 61.84, whereas  
 471 combining it with our proposed Continuous Accuracy (Cont. Acc) reward boosts the score signifi-  
 472 cantly to 72.20, indicating both components are crucial. Furthermore, the study validates the su-  
 473 periority of our continuous reward design over a standard binary alternative. A model using a simple  
 474 binary accuracy reward (Acc + Format), which provides a sparse correct/incorrect signal, is clearly  
 475 outperformed by our model using the continuous reward (Cont. Acc + Format). This demonstrates  
 476 the effectiveness of our quadratic reward function, which provides a dense and informative learning  
 477 gradient. By rewarding "nearly correct" answers, it encourages the fine-grained improvements in  
 478 visual estimation necessary for achieving higher precision.  
 479

#### 5.4 CASE STUDY

480 In Figure 3, powerful models like GPT-4o and Qwen2.5-VL-7B either misinterpret the query or  
 481 resort to factual hallucination. In contrast, our ChartVR, sculpted by the RFT strategy, demon-  
 482 strates a flawless, step-by-step reasoning process. This case study provides a compelling visual proof of our  
 483 quantitative findings: ChartVR enhanced by the RFT strategy is transformed from a system prone  
 484 to errors and hallucination into a reliable and structured visual reasoner that moves beyond merely  
 485 optimizing for the answer.

Table 5: Ablation study of reward function components for Qwen2.5-VL-7B.

<b>Reward Component</b>	<b>Score</b>
Format	61.84
Cont. Acc	67.88
Acc + Format	70.28
<b>Cont. Acc + Format</b>	<b>72.20</b>

486 

## 6 CONCLUSION

488 In this paper, we investigate a compelling yet significant question: "Do MLLMs really understand the charts?" By establishing the ChartVRBench, we extensively evaluated open-source, close-  
 489 source, and chart-specific MLLMs. The results shows a significant degradation in the performance  
 490 of these models, and, through chain-of-thought reasoning, revealed their inability to estimate numerical  
 491 values through visual reasoning, similar to human behavior. To address this issue, we propose  
 492 ChartVR, which enhances the visual reasoning ability of MLLMs via an RFT strategy. This strategy  
 493 first activates reasoning capabilities through SFT, and then generalizes reasoning abilities through  
 494 RL. Extensive experiments conducted on the proposed ChartVRBench and public chart reasoning  
 495 datasets demonstrate the effectiveness of ChartVR. This work paves the way for empowering  
 496 MLLMs to really understand the charts in a human-like manner.  
 497

498 

## ETHICS STATEMENT

501 This research adheres to the ICLR Code of Ethics. The *ChartVRBench* dataset was constructed with  
 502 ethical considerations as a priority, with real-world chart data sourced exclusively from publicly  
 503 accessible platforms (Statista and Our World in Data) in strict adherence to their terms of service.  
 504 Human participation was limited to the ethical recruitment and fair compensation of annotators for  
 505 the curation of question-answer pairs and for a small-scale study to calibrate our human-aligned  
 506 evaluation metric. The purpose of all tasks was clearly communicated. We believe our work, which  
 507 aims to foster more reliable and less hallucinatory AI systems by promoting genuine visual reasoning,  
 508 does not raise any major negative societal concerns.  
 509

510 

## REPRODUCIBILITY STATEMENT

512 To ensure the full reproducibility of our findings, all code, data, and trained models will be made  
 513 publicly available upon publication. The source code for our novel Reinforcement Finetuning (RFT)  
 514 framework, including implementations for both the SFT and GRPO stages, along with all evaluation  
 515 scripts, will be released. The complete *ChartVRBench* dataset, including data generation scripts  
 516 for the synthetic portion, will also be made available. Detailed descriptions of the data curation  
 517 process, training hyperparameters, and evaluation protocols are provided in Appendices A, B, and  
 518 C, respectively. Finally, we will release the final weights for our trained ChartVR-3B and ChartVR-  
 519 7B models to facilitate future research.  
 520

521 

## LLM USAGE STATEMENT

523 LLMs were utilized as general-purpose assistants throughout this research project. In the research  
 524 phase, LLMs served as a tool to accelerate our workflow by generating professional experiment  
 525 code, assisting with bug fixing, and conducting deep research to help discover novel ideas and related  
 526 works. During the preparation of this manuscript, LLM was also used as a writing and editing  
 527 assistant to polish prose for clarity, improve the narrative flow of sections, and format complex  
 528 LaTeX tables. All scientific claims, data analysis, and final conclusions were determined by the  
 529 human authors, who have reviewed all generated and modified content to ensure its correctness and  
 530 take full responsibility for the scientific integrity of this paper.  
 531

532 

## REFERENCES

534 Shuai Bai, Keqin Chen, Xuejing Liu, Jialin Wang, Wenbin Ge, Sibo Song, Kai Dang, Peng Wang,  
 535 Shijie Wang, Jun Tang, et al. Qwen2.5-vl technical report, 2025. URL <https://arxiv.org/abs/2502.13923>.  
 537  
 538 Lei Chen, Xuanle Zhao, Zhixiong Zeng, Jing Huang, Yufeng Zhong, and Lin Ma. Chart-r1: Chain-  
 539 of-thought supervision and reinforcement for advanced chart reasoner, 2025. URL <https://arxiv.org/abs/2507.15509>.  
 540

540 Gheorghe Comanici, Eric Bieber, Mike Schaeckermann, Ice Pasupat, Noveen Sachdeva, Inderjit  
 541 Dhillon, Marcel Blistein, Ori Ram, Dan Zhang, Evan Rosen, et al. Gemini 2.5: Pushing the  
 542 frontier with advanced reasoning, multimodality, long context, and next generation agentic capa-  
 543 bilities, 2025. URL <https://arxiv.org/abs/2507.06261>.

544 DeepSeek-AI, Daya Guo, Dejian Yang, Haowei Zhang, Junxiao Song, Ruoyu Zhang, Runxin Xu,  
 545 Qihao Zhu, Shirong Ma, Peiyi Wang, et al. Deepseek-r1: Incentivizing reasoning capability in  
 546 llms via reinforcement learning, 2025. URL <https://arxiv.org/abs/2501.12948>.

547 Kaituo Feng, Kaixiong Gong, Bohao Li, Zonghao Guo, Yibing Wang, Tianshuo Peng, Junfei Wu,  
 548 Xiaoying Zhang, Benyou Wang, and Xiangyu Yue. Video-r1: Reinforcing video reasoning in  
 549 mllms, 2025. URL <https://arxiv.org/abs/2503.21776>.

550 Yucheng Han, Chi Zhang, Xin Chen, Xu Yang, Zhibin Wang, Gang Yu, Bin Fu, and Hanwang  
 551 Zhang. Chartllama: A multimodal llm for chart understanding and generation, 2023. URL  
 552 <https://arxiv.org/abs/2311.16483>.

553 Wei He, Zhiheng Xi, Wanxu Zhao, Xiaoran Fan, Yiwen Ding, Zifei Shan, Tao Gui, Qi Zhang,  
 554 and Xuanjing Huang. Distill visual chart reasoning ability from llms to mllms, 2024. URL  
 555 <https://arxiv.org/abs/2410.18798>.

556 Muye Huang, Lai Han, Xinyu Zhang, Wenjun Wu, Jie Ma, Lingling Zhang, and Jun Liu. Evochart:  
 557 A benchmark and a self-training approach towards real-world chart understanding, 2024. URL  
 558 <https://arxiv.org/abs/2409.01577>.

559 Wenzuan Huang, Bohan Jia, Zijie Zhai, Shaosheng Cao, Zheyu Ye, Fei Zhao, Zhe Xu, Yao Hu, and  
 560 Shaohui Lin. Vision-r1: Incentivizing reasoning capability in multimodal large language models,  
 561 2025. URL <https://arxiv.org/abs/2503.06749>.

562 Haotian Liu, Chunyuan Li, Qingyang Wu, and Yong Jae Lee. Visual instruction tuning. In  
 563 A. Oh, T. Naumann, A. Globerson, K. Saenko, M. Hardt, and S. Levine (eds.), *Advances in  
 564 Neural Information Processing Systems*, volume 36, pp. 34892–34916. Curran Associates, Inc.,  
 565 2023. URL [https://proceedings.neurips.cc/paper\\_files/paper/2023/file/6dcf277ea32ce3288914faf369fe6de0-Paper-Conference.pdf](https://proceedings.neurips.cc/paper_files/paper/2023/file/6dcf277ea32ce3288914faf369fe6de0-Paper-Conference.pdf).

566 Shiyin Lu, Yang Li, Qing-Guo Chen, Zhao Xu, Weihua Luo, Kaifu Zhang, and Han-Jia Ye. Ovis:  
 567 Structural embedding alignment for multimodal large language model, 2024. URL <https://arxiv.org/abs/2405.20797>.

568 Ahmed Masry, Do Xuan Long, Jia Qing Tan, Shafiq Joty, and Enamul Hoque. ChartQA: A bench-  
 569 mark for question answering about charts with visual and logical reasoning. In Smaranda Mure-  
 570 san, Preslav Nakov, and Aline Villavicencio (eds.), *Findings of the Association for Computational  
 571 Linguistics: ACL 2022*, pp. 2263–2279, Dublin, Ireland, May 2022. Association for Compu-  
 572 tational Linguistics. doi: 10.18653/v1/2022.findings-acl.177. URL <https://aclanthology.org/2022.findings-acl.177/>.

573 Ahmed Masry, Mehrad Shahmohammadi, Md Rizwan Parvez, Enamul Hoque, and Shafiq Joty.  
 574 ChartInstruct: Instruction tuning for chart comprehension and reasoning. In Lun-Wei Ku, Andre  
 575 Martins, and Vivek Srikumar (eds.), *Findings of the Association for Computational Linguistics:  
 576 ACL 2024*, pp. 10387–10409, Bangkok, Thailand, August 2024. Association for Compu-  
 577 tational Linguistics. doi: 10.18653/v1/2024.findings-acl.619. URL <https://aclanthology.org/2024.findings-acl.619/>.

578 Ahmed Masry, Mohammed Saidul Islam, Mahir Ahmed, Aayush Bajaj, Firoz Kabir, Aaryaman  
 579 Kartha, Md Tahmid Rahman Laskar, Mizanur Rahman, Shadikur Rahman, Mehrad Shahmo-  
 580 hammadi, Megh Thakkar, Md Rizwan Parvez, Enamul Hoque, and Shafiq Joty. ChartQAPro:  
 581 A more diverse and challenging benchmark for chart question answering. In Wanxiang Che,  
 582 Joyce Nabende, Ekaterina Shutova, and Mohammad Taher Pilehvar (eds.), *Findings of the As-  
 583 sociation for Computational Linguistics: ACL 2025*, pp. 19123–19151, Vienna, Austria, July  
 584 2025a. Association for Computational Linguistics. ISBN 979-8-89176-256-5. URL <https://aclanthology.org/2025.findings-acl.978/>.

594 Ahmed Masry, Abhay Puri, Masoud Hashemi, Juan A. Rodriguez, Megh Thakkar, Khyati Maha-  
 595 jan, Vikas Yadav, Sathwik Tejaswi Madhusudhan, Alexandre Piché, Dzmitry Bahdanau, Christo-  
 596 pher Pal, David Vazquez, Enamul Hoque, Perouz Taslakian, Sai Rajeswar, and Spandana Gella.  
 597 *Bigcharts-r1: Enhanced chart reasoning with visual reinforcement finetuning*. In *Second Con-  
 598 ference on Language Modeling*, 2025b. URL <https://openreview.net/forum?id=19fydz1QnW>.

600 Ahmed Masry, Megh Thakkar, Aayush Bajaj, Aaryaman Kartha, Enamul Hoque, and Shafiq Joty.  
 601 *ChartGemma: Visual instruction-tuning for chart reasoning in the wild*. In Owen Rambow, Leo  
 602 Wanner, Marianna Apidianaki, Hend Al-Khalifa, Barbara Di Eugenio, Steven Schockaert, Ka-  
 603 reem Darwish, and Apoorv Agarwal (eds.), *Proceedings of the 31st International Conference  
 604 on Computational Linguistics: Industry Track*, pp. 625–643, Abu Dhabi, UAE, January 2025c.  
 605 Association for Computational Linguistics. URL <https://aclanthology.org/2025.coling-industry.54/>.

606 Nitesh Methani, Pritha Ganguly, Mitesh M. Khapra, and Pratyush Kumar. *Plotqa: Reasoning over  
 607 scientific plots*. In *2020 IEEE Winter Conference on Applications of Computer Vision (WACV)*,  
 608 pp. 1516–1525, 2020. doi: 10.1109/WACV45572.2020.9093523.

609 Srijita Mukhopadhyay, Adnan Qidwai, Aparna Garimella, Pritika Ramu, Vivek Gupta, and Dan Roth.  
 610 *Unraveling the truth: Do VLMs really understand charts? a deep dive into consistency and robust-  
 611 ness*. In Yaser Al-Onaizan, Mohit Bansal, and Yun-Nung Chen (eds.), *Findings of the Association  
 612 for Computational Linguistics: EMNLP 2024*, pp. 16696–16717, Miami, Florida, USA, Novem-  
 613 ber 2024. Association for Computational Linguistics. doi: 10.18653/v1/2024.findings-emnlp.973.  
 614 URL <https://aclanthology.org/2024.findings-emnlp.973/>.

615 OpenAI, :, Aaron Hurst, Adam Lerer, Adam P. Goucher, Adam Perelman, Aditya Ramesh, Aidan  
 616 Clark, AJ Ostrow, Akila Welihinda, Alan Hayes, et al. *Gpt-4o system card*, 2024a. URL <https://arxiv.org/abs/2410.21276>.

617 OpenAI, :, Aaron Jaech, Adam Kalai, Adam Lerer, Adam Richardson, Ahmed El-Kishky, Aiden  
 618 Low, Alec Helyar, Aleksander Madry, Alex Beutel, et al. *Openai o1 system card*, 2024b. URL  
 619 <https://arxiv.org/abs/2412.16720>.

620 Long Ouyang, Jeffrey Wu, Xu Jiang, Diogo Almeida, Carroll Wainwright, Pamela Mishkin, Chong  
 621 Zhang, Sandhini Agarwal, Katarina Slama, Alex Gray, John Schulman, Jacob Hilton, Fraser Kel-  
 622 ton, Luke Miller, Maddie Simens, Amanda Askell, Peter Welinder, Paul Christiano, Jan Leike,  
 623 and Ryan Lowe. *Training language models to follow instructions with human feedback*. In  
 624 Alice H. Oh, Alekh Agarwal, Danielle Belgrave, and Kyunghyun Cho (eds.), *Advances in Neu-  
 625 ral Information Processing Systems*, 2022. URL <https://openreview.net/forum?id=TG8KACxEON>.

626 John Schulman, Filip Wolski, Prafulla Dhariwal, Alec Radford, and Oleg Klimov. *Proximal policy  
 627 optimization algorithms*, 2017. URL <https://arxiv.org/abs/1707.06347>.

628 Zhihong Shao, Peiyi Wang, Qihao Zhu, Runxin Xu, Junxiao Song, Xiao Bi, Haowei Zhang,  
 629 Mingchuan Zhang, Y. K. Li, Y. Wu, and Daya Guo. *Deepseekmath: Pushing the limits of mathe-  
 630 matical reasoning in open language models*, 2024. URL <https://arxiv.org/abs/2402.03300>.

631 Huajie Tan, Yuheng Ji, Xiaoshuai Hao, Minglan Lin, Pengwei Wang, Zhongyuan Wang, and  
 632 Shanghang Zhang. *Reason-rft: Reinforcement fine-tuning for visual reasoning*, 2025. URL  
 633 <https://arxiv.org/abs/2503.20752>.

634 Liyan Tang, Grace Kim, Xinyu Zhao, Thom Lake, Wenxuan Ding, Fangcong Yin, Prasann Singhal,  
 635 Manya Wadhwa, Zeyu Leo Liu, Zayne Sprague, Ramya Namuduri, Bodun Hu, Juan Diego Ro-  
 636 driguez, Puyuan Peng, and Greg Durrett. *Chartmuseum: Testing visual reasoning capabilities of  
 637 large vision-language models*, 2025a. URL <https://arxiv.org/abs/2505.13444>.

638 Liyan Tang, Shreyas Pimpalgaonkar, Kartik Sharma, Alexandros G. Dimakis, Mahesh Sathiamoorthy,  
 639 and Greg Durrett. *Bespoke-minichart-7b: pushing the frontiers of open vlms for chart  
 640 understanding*. blog post, 2025b. URL <https://huggingface.co/bespokelabs/Bespoke-MiniChart-7B>.

648 Gemma Team, Aishwarya Kamath, Johan Ferret, Shreya Pathak, Nino Vieillard, Ramona Merhej,  
 649 Sarah Perrin, Tatiana Matejovicova, Alexandre Ramé, Morgane Rivière, et al. Gemma 3 technical  
 650 report, 2025. URL <https://arxiv.org/abs/2503.19786>.

651

652 Yizhong Wang, Yeganeh Kordi, Swaroop Mishra, Alisa Liu, Noah A. Smith, Daniel Khashabi, and  
 653 Hannaneh Hajishirzi. Self-instruct: Aligning language models with self-generated instructions.  
 654 In Anna Rogers, Jordan Boyd-Graber, and Naoaki Okazaki (eds.), *Proceedings of the 61st Annual  
 655 Meeting of the Association for Computational Linguistics (Volume 1: Long Papers)*, pp. 13484–  
 656 13508, Toronto, Canada, July 2023. Association for Computational Linguistics. doi: 10.18653/  
 657 v1/2023.acl-long.754. URL <https://aclanthology.org/2023.acl-long.754/>.

658

659 Zirui Wang, Mengzhou Xia, Luxi He, Howard Chen, Yitao Liu, Richard Zhu, Kaiqu Liang, Xindi  
 660 Wu, Haotian Liu, Sadhika Malladi, Alexis Chevalier, Sanjeev Arora, and Danqi Chen. Charxiv:  
 661 Charting gaps in realistic chart understanding in multimodal LLMs. In *The Thirty-eight Confer-  
 662 ence on Neural Information Processing Systems Datasets and Benchmarks Track*, 2024. URL  
<https://openreview.net/forum?id=cy8mq7QYae>.

663

664 Renqiu Xia, Bo Zhang, Hancheng Ye, Xiangchao Yan, Qi Liu, Hongbin Zhou, Zijun Chen, Peng Ye,  
 665 Min Dou, Botian Shi, Junchi Yan, and Yu Qiao. Chartx & chartvlm: A versatile benchmark and  
 666 foundation model for complicated chart reasoning, 2025. URL <https://arxiv.org/abs/2402.12185>.

667

668 Can Xu, Qingfeng Sun, Kai Zheng, Xiubo Geng, Pu Zhao, Jiazhan Feng, Chongyang Tao, Qingwei  
 669 Lin, and Daxin Jiang. Wizardlm: Empowering large pre-trained language models to follow com-  
 670 plex instructions. In *The Twelfth International Conference on Learning Representations*, 2024a.

671

672 Zhengzhuo Xu, Sinan Du, Yiyan Qi, Chengjin Xu, Chun Yuan, and Jian Guo. Chartbench: A  
 673 benchmark for complex visual reasoning in charts, 2024b. URL <https://arxiv.org/abs/2312.15915>.

674

675 Liang Zhang, Anwen Hu, Haiyang Xu, Ming Yan, Yichen Xu, Qin Jin, Ji Zhang, and Fei  
 676 Huang. TinyChart: Efficient chart understanding with program-of-thoughts learning and vi-  
 677 sual token merging. In Yaser Al-Onaizan, Mohit Bansal, and Yun-Nung Chen (eds.), *Pro-  
 678 ceedings of the 2024 Conference on Empirical Methods in Natural Language Processing*, pp.  
 679 1882–1898, Miami, Florida, USA, November 2024. Association for Computational Linguis-  
 680 tics. doi: 10.18653/v1/2024.emnlp-main.112. URL [https://aclanthology.org/2024.emnlp-main.112/](https://aclanthology.org/2024.emnlp-main.112).

681

682 Yuze Zhao, Jintao Huang, Jinghan Hu, Xingjun Wang, Yunlin Mao, Daoze Zhang, Zeyinzi Jiang,  
 683 Zhikai Wu, Baole Ai, Ang Wang, et al. Swift: a scalable lightweight infrastructure for fine-tuning.  
 684 In *Proceedings of the AAAI Conference on Artificial Intelligence*, volume 39, pp. 29733–29735,  
 2025.

685

686 Jinguo Zhu, Weiyun Wang, Zhe Chen, Zhaoyang Liu, Shenglong Ye, Lixin Gu, Hao Tian, Yuchen  
 687 Duan, Weijie Su, Jie Shao, et al. Internvl3: Exploring advanced training and test-time recipes for  
 688 open-source multimodal models, 2025. URL <https://arxiv.org/abs/2504.10479>.

689

690

691

692

693

694

695

696

697

698

699

700

701

702 APPENDIX  
703

704 • Sec. A provides details of the proposed benchmark, *ChartVRBench*, including the problem  
705 definition, data sources, topics, and chart types.  
706 • Sec. B describes the training strategy of the *ChartVR*, detailing the construction of the SFT and  
707 RL datasets.  
708 • Sec. C presents further details on the evaluation and inference.  
709 • Sec. D interpret the human performance in ChartVRBench.  
710

712 A CHARTVRBENCH BENCHMARK DETAILS  
713714 A.1 PROBLEM DEFINITION  
715

716 The primary task addressed by our benchmark, *ChartVRBench*, is numerical value estimation on  
717 non-annotated charts. Formally, given a chart image  $C$  and a query  $Q$  that specifies a target data  
718 point within the chart, the goal is to produce a numerical answer  $A$  that accurately estimates the  
719 value of that data point. Crucially, the chart image  $C$  is non-annotated, meaning that the numerical  
720 values corresponding to graphical elements (e.g., the height of a bar, a point on a line) are not present  
721 as explicit text labels.

722 This task is fundamentally a visual reasoning problem, rather than a simple recognition or textual  
723 reasoning task. To arrive at the correct answer  $A$ , a model cannot only rely on Optical Character  
724 Recognition (OCR). Instead, it must perform a multi-step cognitive process grounded in the visual  
725 geometry of the chart:

726 1. Semantic Understanding & Grounding: The model must first parse the query  $Q$  and correctly  
727 associate the textual description with the corresponding graphical elements in the chart image  $C$   
728 (e.g., a specific bar, a specific colored line).  
729 2. Structural and Scale Interpretation: The model must identify and interpret the chart's structural  
730 components, particularly the relevant axes (e.g., the y-axis) and their numerical scales, including  
731 the range and the value represented by tick marks and grid lines.  
732 3. Spatial and Proportional Reasoning: Finally, the model must perform spatial reasoning by com-  
733 paring the target graphical element's dimension (e.g., its height or position) against the inter-  
734 preted scale of the axis. This often requires proportional estimation or interpolation between  
735 labeled tick marks to infer the final numerical value.  
736

737 By designing a task that necessitates this entire reasoning chain, we directly evaluate a model's  
738 ability to not just *recognize* a chart, but to truly *understand* its underlying quantitative information.  
739

741 A.2 DATA TOPICS AND CHART EXAMPLES  
742

743 To ensure the breadth relevance of *ChartVRBench*, the synthetic data generation process samples  
744 from a diverse set of 38 distinct topics, as shown in Table 6 guaranteeing that the charts cover a  
745 variety of contexts and narratives. Furthermore, to robustly evaluate a model's visual reasoning  
746 capabilities across different graphical representations, ChartVRBench incorporates seven primary  
747 chart types. Figure 5 provides a representative example for each of these types, showcasing the  
748 visual diversity and complexity present in our benchmark.

750 A.3 REAL-WORLD CHART COLLECTION  
751

752 To ensure *ChartVRBench* reflects the challenges of real-world applications, we curated a substantial  
753 collection of charts from public online sources. This section details our three-stage process: data  
754 sourcing, a rigorous manual filtering protocol, and a hybrid human-AI pipeline for generating high-  
755 quality question-answer pairs. Figure 6 showcases several examples of the final curated real-world  
charts from our collection.

756 Table 6: The 38 topics covered in the ChartVRBench dataset.  
757

758 Category	759 Category
760 Agriculture and Food Production	Human Resources and Employee Management
761 Architecture and Building	Language and Communication
762 Artificial Intelligence and Robotics	Law and Legal Affairs
763 Art and Design	Literature and Writing
764 Astronomy and Space	Manufacturing and Production
765 Biology and Life Sciences	Marketing and Advertising
766 Books and Publishing	Mathematics and Statistics
767 Business and Finance	Music and Performance
768 Computer Science and Information Technology	Physics and Chemistry
769 Education and Academics	Real Estate and Housing Market
770 Energy and Utilities	Religion and Spirituality
771 Environment and Sustainability	Retail and E-commerce
772 Fashion and Style	Science and Engineering
773 Film and Cinema	Social Media and the Web
774 Food and Beverage Industry	Social Sciences and Humanities
775 Futurism and Innovation	Society and Community
776 Government and Public Policy	Sports and Entertainment
777 Healthcare and Health	Transportation and Logistics
778 History and Culture	Travel and Exploration

## 779 A.3.1 DATA SOURCING

780 **Statista.** A significant portion of the real-world charts was sourced from Statista<sup>2</sup>, a leading global  
781 platform specializing in market and consumer data. Statista provides professional, data-driven vi-  
782 sualizations for a wide array of industries, covering topics from economic indicators and market  
783 forecasts to technology trends and consumer behavior.

784 **Our World in Data.** The second major source was Our World in Data<sup>3</sup>, a renowned scientific  
785 online publication based at the University of Oxford. Its mission is to make data and research on the  
786 world’s most significant challenges, such as global health, economic development, and environmen-  
787 tal change, accessible and understandable through complex and data-rich visualizations.

788 In addition to these two primary repositories, the collection was supplemented by charts from various  
789 other miscellaneous public reports and online publications. All data collection was conducted in  
790 strict adherence to the copyright policies, terms of service, and licensing agreements of each source  
791 to ensure full ethical compliance.

## 792 A.3.2 CURATION PROTOCOL

793 Once a large pool of charts was collected, each candidate chart underwent a meticulous, two-step  
794 curation process performed by our recruited team of human annotators.

795 **Step 1: Manual Filtering and Vetting.** Each chart was manually vetted against stringent crite-  
796 ria for inclusion in *ChartVRBench*. A chart was accepted only if it satisfied all of the following  
797 conditions, otherwise it was discarded:

- 802 1. High Visual Quality: The image must be of sufficient resolution, clear, and free of significant  
803 compression artifacts or other visual noise that could impede interpretation.
- 804 2. Data Integrity: The chart must be coherent and visually consistent, with clearly defined axes,  
805 legends, and graphical elements.
- 806 3. Absence of Annotations: We exclusively select charts where numerical values are not explicitly  
807 printed on the graphical elements (e.g., no numbers on top of bars). This constraint is funda-  
808

809 <sup>2</sup><https://www.statista.com/><sup>3</sup><https://ourworldindata.org/>

810  
811  
812  
813  
814  
815  
816  
817  
818  
819  
820  
821  
822  
823  
824  
825  
826  
827  
828  
829  
830  
831  
832  
833  
834  
835  
836  
837  
838  
839  
840  
841  
842  
843  
844  
845  
846  
847  
848  
849  
850  
851  
852  
853  
854  
855  
856  
857  
858  
859  
860  
861  
862  
863

mental to our benchmark, as it forces a model to perform genuine visual reasoning rather than relying on OCR shortcuts.

**Step 2: Question-Answer Pair Generation.** Once a chart was approved, we employed a two-stage, human-in-the-loop process to generate its corresponding question-answer pair:

1. **MLLM-based Candidate Generation:** We first use a capable MLLM to generate an initial set of candidate question-answer pairs for each chart, prompting it to ask a specific numerical estimation question.
2. **Human Verification and Refinement:** Every MLLM-generated pair is then subjected to rigorous human review. Annotators verify the question’s clarity and relevance, and then carefully perform the visual estimation themselves to validate the answer’s accuracy. If necessary, they refine the question’s phrasing or correct the ground-truth answer to ensure the final Q&A pair is unambiguous and factually correct.

## B DETAILS OF DATASETS AND TRAINING

### B.1 DATA CONSTRUCTION FOR SFT

The dataset used for the Supervised Fine-Tuning (SFT) “cold start” phase is meticulously constructed through a **knowledge distillation** process. The goal is to generate high-quality Chain-of-Thought (CoT) data that can effectively activate the reasoning paradigm of our base models.

While we utilize the same underlying generation pipeline (rendering engine and topic distribution) to ensure domain consistency, the specific chart instances and question-answer pairs in the SFT set are distinct from those in the benchmark. Crucially, to maintain strict train-test separation, this SFT dataset is generated as a completely independent batch from the ChartVRBench evaluation set.

This process leverages a powerful teacher model (Qwen2.5-VL-32B-Instruct) to generate reasoning traces for this training-specific corpus. The data construction pipeline involves several key stages to ensure the quality and validity of the final CoT samples:

1. **Prompting for Chain-of-Thought Generation:** For each generated training instance, consisting of Python plotting code ( $C$ ) and a question ( $Q$ ), we employ the teacher LLM to generate a step-by-step reasoning process. The core of this process involves a carefully constructed textual prompt that integrates the Python code ( $C$ ) and the question ( $Q$ ). This prompt is designed to force the model to articulate a logical pathway from the code and question to the correct result. The model is required to structure its output using specific tags, separating the reasoning steps ( $<\text{think}>\dots</\text{think}>$ ) from the final answer ( $<\text{answer}>\dots</\text{answer}>$ ).
2. **Validation and Filtering:** Each generated CoT sample undergoes a rigorous, multi-step validation process to filter out low-quality or incorrect reasoning:
  - **Structural Check:** The generated text is first parsed to ensure that both the reasoning and answer tags are present. Samples with missing tags are discarded.
  - **Answer Verification:** The final answer extracted from the  $<\text{answer}>$  tag is programmatically compared against the ground-truth answer derived from the code. We employ a robust evaluation function that checks for both exact string matches and numerical equivalence within a tolerance threshold to ensure correctness.
  - **Leakage Detection:** The generated reasoning trace within the  $<\text{think}>$  tags is scanned for any mention of the “original answer.” This crucial step prevents the model from “cheating” by simply copying the ground-truth answer into its reasoning, ensuring that the generated thought process is genuine.

### B.2 RL ALGORITHM SELECTION

We selected GRPO to fine-tune our multimodal model for enhanced chart visual reasoning, primarily due to its superior efficiency and its alignment with our reward structure. Compared to Proximal Policy Optimization (PPO), GRPO significantly reduces computational and memory overhead. GRPO eliminates the need for a separate value model—which is typically as large as the policy model—by

864 estimating the baseline directly from the scores of multiple sampled outputs. This efficiency is criti-  
 865 cal given the large scale of our models (e.g., 7B parameters), making GRPO a practical solution  
 866 under limited hardware resources.

867 Furthermore, while Direct Preference Optimization (DPO) offers an efficient alternative to tradi-  
 868 tional RLHF, it is fundamentally designed for binary preference datasets (i.e., chosen vs. rejected  
 869 responses). Our task, however, benefits from a more granular, continuous reward signal that reflects  
 870 the degree of correctness in quantitative analysis. GRPO is adept at directly optimizing for such  
 871 programmatic, scalar rewards, allowing the model to learn from fine-grained feedback. This makes  
 872 it better suited for improving the visual reasoning in chart than a preference-based method like DPO.  
 873

### 874 B.3 DATASET CONSTRUCTION FOR GRPO

875 The curation process, inspired by the principles of rejection sampling and active learning, involves a  
 876 multi-round, varied-prompting inference pipeline designed to probe the model’s knowledge bound-  
 877 aries. The goal of this pipeline is to construct a specialized, high-signal dataset by isolating ambigui-  
 878 ous cases that the SFT-tuned model can sometimes solve but not consistently. This strategy focuses  
 879 the training process on the most informative examples where the model is most uncertain, rather  
 880 than wasting computational resources on problems that are already mastered (always correct) or are  
 881 currently too difficult (always incorrect).

882 Our pipeline involves the following systematic steps:

- 883 1. **Initial Dataset Curation:** We begin by constructing an initial, high-quality dataset for GRPO.  
 884 This dataset is synthesized following the method introduced earlier. We selected only those  
 885 instances that achieved a score of either 4 or 5, ensuring a strong baseline of correct.
- 886 2. **Multi-Round Inference:** Initially, we run inference multiple times on the initial GRPO dataset  
 887 using our base model. To elicit a wide range of reasoning pathways and outcomes for each  
 888 problem, we set the sampling temperature to 1.0 for each run.
- 889 3. **Filtering for "Stochastic Correctness":** The correctness of every generated response is logged.  
 890 After all rounds are complete, we filter this log to isolate the target samples. We select only those  
 891 question-answer pairs that the model answered correctly in at least one round but incorrectly in  
 892 at least one other round.

893 The rationale behind this selective filtering is to force the policy to learn to distinguish between suc-  
 894 cessful and flawed reasoning pathways for the exact same problem. Training on these "boundary"  
 895 cases ensures that the GRPO stage is dedicated to resolving ambiguity and reinforcing robust rea-  
 896 soning where it is most needed, leading to more significant and generalizable improvements in the  
 897 model’s core abilities.

### 901 B.4 DETAILED FORMULATION OF THE ACCURACY REWARD

902 A core component of the GRPO framework is the **Continuous Accuracy Reward** ( $R_{acc}$ ), which is  
 903 designed to provide a dense, fine-grained signal for optimizing the model’s numerical estimation  
 904 capabilities. A simple binary reward (correct/incorrect) is often too sparse for reinforcement learning,  
 905 as it fails to differentiate between a near-miss and a completely wrong answer. To overcome this,  
 906 we designed a continuous reward function that recognizes and rewards "nearly correct" answers,  
 907 thereby creating a smoother optimization landscape.

908 Our accuracy reward function provides a dense, informative, and well-behaved signal that is ide-  
 909 ally suited for guiding our reinforcement learning process towards generating highly accurate and  
 910 reliable numerical estimations.

### 911 B.5 MORE TRAINING DETAILS

912 Our training process begins with the Qwen2.5-VL-7B-Instruct model as the foundation. Using the  
 913 Swift framework, we perform SFT for 2 epochs on our 4.2k instruction-following dataset. In this  
 914 stage we freeze the vision tower and the multimodal aligner while exclusively tuning the LLM’s  
 915 parameters. We set the learning rate to 1e-5 with a warm-up ratio of 0.05 and use an effective batch

918 size of 256. The SFT process is conducted on 8 NVIDIA H800 GPUs, utilizing bfloat16 precision  
 919 and the DeepSpeed ZeRO-3 optimization strategy.  
 920

921 For the GRPO stage, we initialize the model with the checkpoint from the SFT phase and employ  
 922 the GRPO algorithm on our 3.4k preference dataset. In this phase, we continue to freeze the vision  
 923 tower but expand the scope of fine-tuning to include both the LLM and the multimodal aligner. The  
 924 learning rate is reduced to 1e-6, again with a 0.05 warm-up ratio. For the rollout process, we use a  
 925 generation batch size of 32 to create 4 completions per sample with a temperature of 1.0; the training  
 926 itself uses an effective batch size of 64. The reward function is the composite of the Format and  
 927 Continuous Accuracy rewards. The hardware and optimization setup remains consistent, utilizing 8  
 928 NVIDIA H800 GPUs with bfloat16 precision and DeepSpeed ZeRO-3.  
 929

## 930 C EVALUATION AND INFERENCE DETAILS

931 This section outlines the precise methodologies and inference settings used to evaluate all models  
 932 and benchmarks, ensuring full reproducibility and fairness. Our protocols were designed by strictly  
 933 adhering to the author-recommended settings and official evaluation scripts where available.  
 934

### 935 C.1 GENERAL INFERENCE SETTINGS

936 All experiments reported in this paper were conducted using the default hyperparameters of each re-  
 937 spective model, with no model-specific tuning performed at inference time. To ensure reproducibil-  
 938 ity, the random seed for all generation processes was fixed to 42, and the sampling temperature  
 939 was set to 1.0. Our inference pipeline is built upon the vLLM framework, which provides efficient,  
 940 high-throughput serving for Large Language Models.  
 941

### 942 C.2 EVALUATION ON CHARTVRBENCH

943 Our evaluation on the proposed ChartVRBench employed different prompting strategies depending  
 944 on the model type to ensure a fair and rigorous assessment.  
 945

946 **General MLLMs.** To verify the visual reasoning capabilities of general-purpose models, we em-  
 947 ployed a structured Chain-of-Thought (CoT) prompt, shown in Figure 10. This prompt compels the  
 948 model to first articulate its reasoning—by analyzing axes, data points, and context—before provid-  
 949 ing a final answer. The prompt enforces a strict separation between the step-by-step logic (output  
 950 in ‘`;think;`’ tags) and the concise final output (in an ‘`;answer;`’ tag). This approach allows us to  
 951 pinpoint the exact stage where a model’s logic succeeds or fails, moving our analysis beyond simple  
 952 accuracy metrics.  
 953

954 **Chart-Specific Models.** In contrast, for models already fine-tuned on specific chart-related data  
 955 formats (including ChartGemma, TinyChart, ChartInstruct, ChartVLM, and ChartLlama), we did  
 956 not use our generalized CoT prompt. To elicit their best possible performance and establish the  
 957 strongest baseline, we followed the official author-recommended procedures:  
 958

- 959 1. We cloned the official public repository for each model.  
 960
- 961 2. We utilized their provided, out-of-the-box inference scripts and default model weights without  
 962 modification.  
 963
- 964 3. We fed the images and questions from our ChartVRBench test set directly into these scripts.  
 965

966 This methodology ensures that we are comparing our model against the most capable version of  
 967 each specialized baseline.  
 968

### 969 C.3 EVALUATION OF CHARTVR ON PUBLIC BENCHMARKS

970 To validate the generalization of *ChartVR*’s enhanced reasoning capabilities, we evaluated it against  
 971 several standard public benchmarks, following the official protocol for each.  
 972

972     **CharXiv.** We utilized the official code and evaluation scripts from the CharXiv repository. We  
 973     integrated our locally-deployed *ChartVR* as the model backend into their inference pipeline, keeping  
 974     all other components (data loading, pre-processing, and scoring scripts) identical to the original  
 975     setup.  
 976

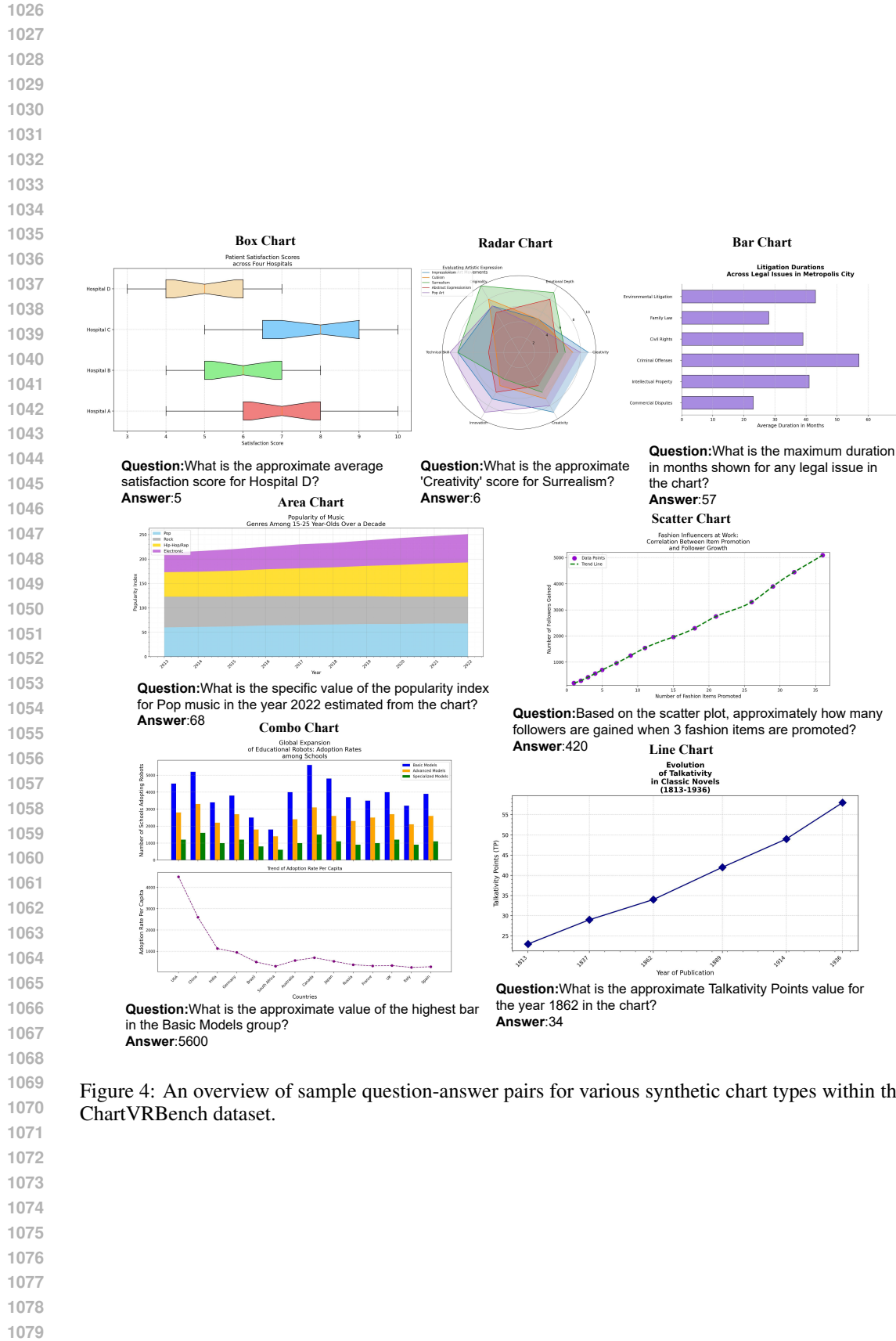
977     **ChartBench.** Our evaluation followed a similar protocol using the complete pipeline from the of-  
 978     ficial ChartBench repository. We generated predictions with our *ChartVR* model and fed the outputs  
 979     directly into the official scoring script.  
 980

981     **ChartQapro.** As the official repository provides a standalone evaluation script but not a full  
 982     inference pipeline, we implemented a two-step process. First, we developed a script to generate  
 983     predictions for the test set using a prompt that precisely replicated the template described in the  
 984     ChartQapro paper. Second, the resulting file of predictions was used as input for the official eval-  
 985     uation script to compute the final accuracy score.  
 986

## 987     D INTERPRETATION OF HUMAN PERFORMANCE

988  
 989     It is important to note that human accuracy on this task is not 100%. This is primarily due to inherent  
 990     tendencies in human visual estimation, for instance, individuals often gravitate towards estimating  
 991     with round or integer values that appear close to the correct answer, rather than performing precise  
 992     interpolation. Our analysis indicates that a 2% relative error tolerance is a reasonable threshold to  
 993     account for these natural human inaccuracies.  
 994

995     Furthermore, performance varies significantly across chart types. For area charts, accuracy sees a  
 996     substantial decline, because many questions require calculating the difference between the upper and  
 997     lower boundaries of a shaded region, a task made considerably more difficult by the common ab-  
 998     sence of horizontal gridlines as visual aids. Similarly, for complex combo charts, lower performance  
 999     can be attributed to cognitive factors, such as misinterpretation of the prompt or misunderstanding  
 1000     the intricate relationships between different chart components.  
 1001  
 1002  
 1003  
 1004  
 1005  
 1006  
 1007  
 1008  
 1009  
 1010  
 1011  
 1012  
 1013  
 1014  
 1015  
 1016  
 1017  
 1018  
 1019  
 1020  
 1021  
 1022  
 1023  
 1024  
 1025



1080

1081

1082

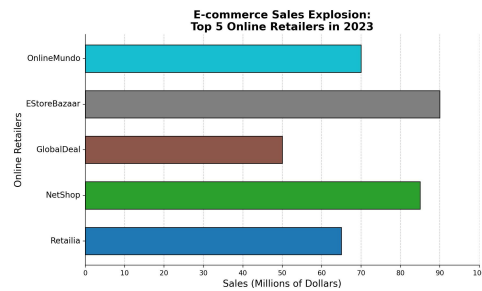
1083

1084

1085

1086

1087



1088

1089

1090

1091

1092

1093

1094

1095

1096

1097

1098

1099

1100

1101

1102

1103

1104

1105

1106

1107

1108

1109

1110

1111

1112

1113

1114

1115

1116

1117

1118

1119

1120

1121

1122

1123

1124

1125

1126

1127

1128

1129

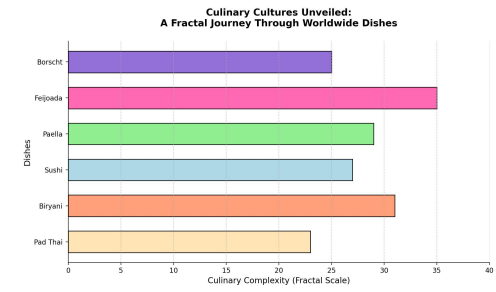
1130

1131

1132

1133

## Bar Chart



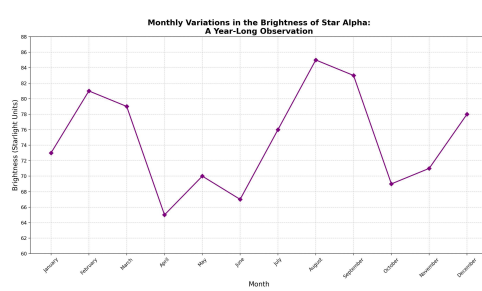
**Question:** What is the approximate sales volume for 'NetShop' in the chart? Please analyze based on the chart coordinates?

**Answer:** 85

**Question:** What is the approximate culinary complexity of Pad Thai as shown on the chart?

**Answer:** 23

## Line Chart



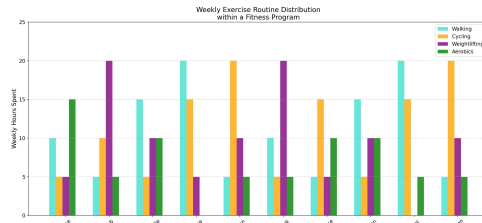
**Question:** What is the approximate brightness value of Star Alpha in August analyzed based on the line chart?

**Answer:** 85

**Question:** What is the specific step count value for the 20th day as shown in the graph?

**Answer:** 7191

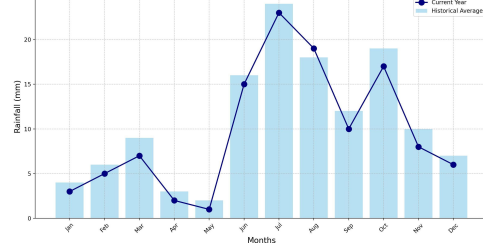
## Combo Chart



**Question:** What is the specific value of the weekly hours spent on Weightlifting by Charlie analyzed based on the coordinate axis?

**Answer:** 10

## Monthly Rainfall Fluctuations in a Tropical Region (Current Year vs Historical Average)



**Question:** What is the historical average rainfall in June based on the chart's coordinate axis?

**Answer:** 16

Figure 5: An overview of sample question-answer pairs for various complex synthetic chart types within the ChartVRBench dataset.

1134

1135

1136

1137

1138

1139

1140

1141

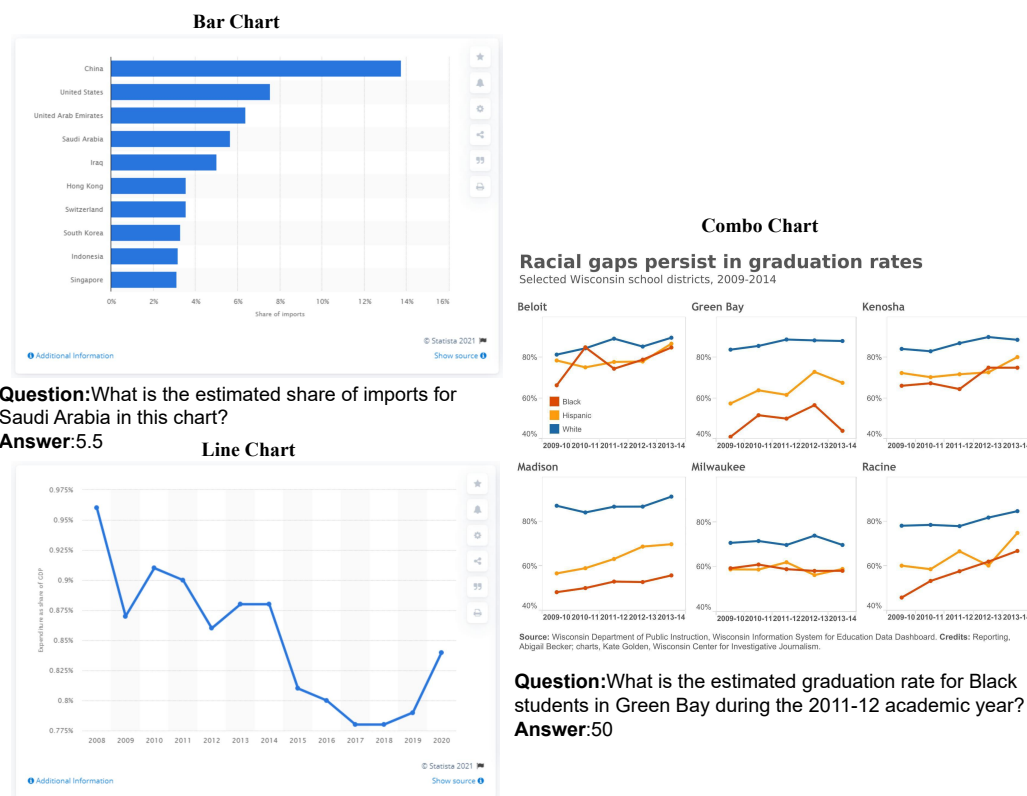
1142

1143

1144

1145

1146



**Question:**What is the estimated share of imports for Saudi Arabia in this chart?

**Answer:**5.5

**Question:**What was the estimated Expenditure as share of GDP for the year 2015?

**Answer:**0.81

Figure 6: An overview of sample question-answer pairs for various real chart types within the ChartVRBench dataset.

1188  
 1189  
 1190  
 1191  
 1192 **Distill CoT Data Prompt:**  
 1193  
 1194 **ROLE**  
 1195  
 1196  
 1197 You are an expert vision-language analyst.  
 1198 Your job is to look at the image, read the question, think  
 1199 step-by-step, and provide the final answer.  
 1200  
 1201 **CRITICAL RULES (must follow all)**  
 1202  
 1203  
 1204 1. **\*\*Use ONLY the image and the question\*\*** when you  
 1205 think.  
 1206   └ The “Original Answer” is supplied **\*\*solely for self-**  
 1207 **checking\*\*.**  
 1208   └ NEVER quote, copy, hint at, or mention it in your  
 1209 reasoning.  
 1210   └ Forbidden words/phrases inside <think>:  
 1211       “original answer”, “ground-truth”, “GT”, “correct  
 1212 answer”, or the answer value itself.  
 1213  
 1214 2. Finish your full reasoning first, then decide your own  
 1215 answer  
 1216   ( $\pm 2\%$  numerical tolerance is acceptable).  
 1217   └ If truly uncertain, output “uncertain” in <answer>.  
 1218  
 1219 3. Output exactly TWO tags in this order—nothing else:  
 1220   <think>Your reasoning here</think>  
 1221   <answer>Your final answer</answer>  
 1222  
 1223 **INPUT FIELDS**  
 1224  
 1225  
 1226 Question : **{original\_question}**  
 1227 Original Answer (for self-check only) : **{original\_answer}**  
 1228  
 1229 **EXAMPLE OUTPUT**  
 1230  
 1231  
 1232  
 1233 <think>The point at “1900-present” lies slightly above the  
 1234 90 tick; reading the y-axis, it corresponds to 93 on the  
 1235 popularity scale.</think>  
 1236 <answer>93</answer>  
 1237  
 1238  
 1239  
 1240  
 1241

Figure 7: The Prompt in Distilling the CoT Data

1242

1243

1244

1245

1246

1247

1248

1249

1250

1251

1252

1253

1254

1255

1256

1257

1258

1259

1260

1261

1262

1263

1264

1265

1266

1267

1268

1269

1270

1271

1272

1273

1274

1275

1276

1277

1278

1279

1280

1281

1282

1283

1284

1285

1286

1287

1288

1289

1290

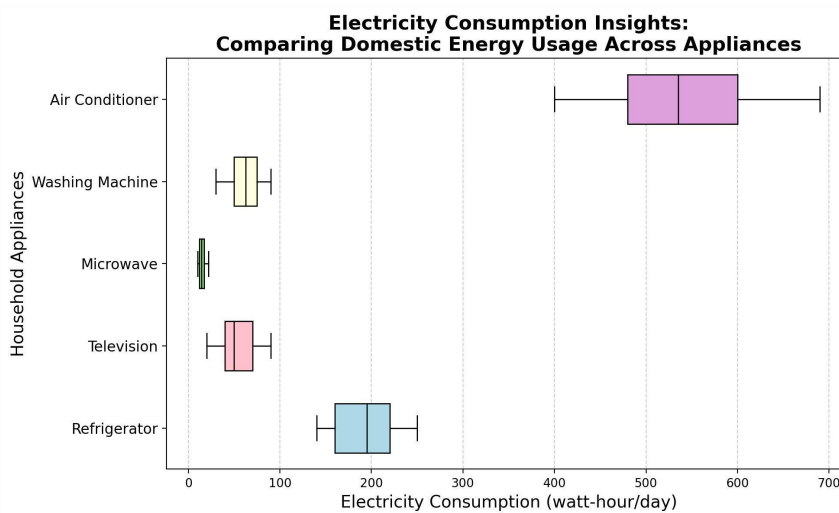
1291

1292

1293

1294

1295



**Question:** What is the median electricity consumption for the **Washing Machine** based on the boxplot coordinates?

**Chart Type:** Box Chart

**Answer:** 60

**CoT Data:** <think>

Step 1: Locate the bar for "**Washing Machine**" on the y-axis, which is positioned in the middle of the chart.

Step 2: Identify the thick horizontal line inside the box of the "Washing Machine" bar. This line represents the median.

Step 3: Follow the median line horizontally to the x-axis, which shows electricity consumption in watt-hour/day.

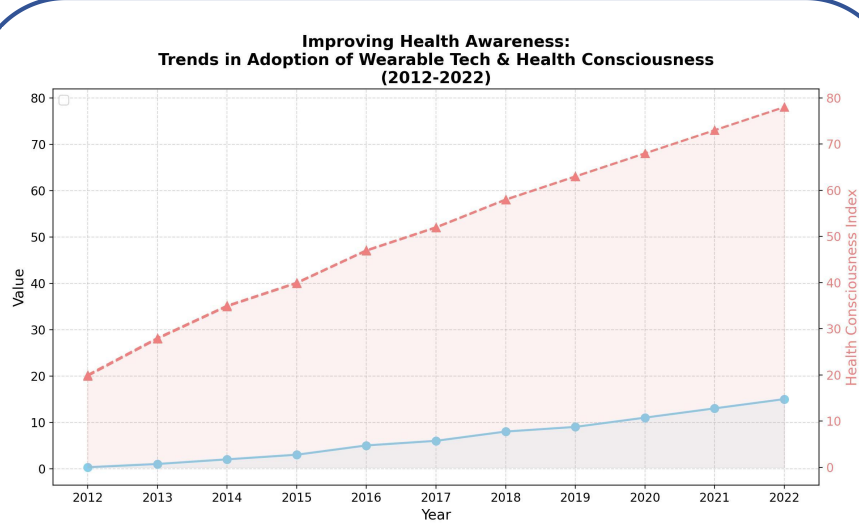
Step 4: The median line intersects the **x-axis at a point that lies exactly on the 60 mark**, as it aligns perfectly with the gridline labeled 60.

Step 5: Giving the Answer is 60.</think>

<answer>60</answer>

Figure 8: Example 1 of CoT Dataset

1296  
 1297  
 1298  
 1299  
 1300  
 1301  
 1302  
 1303  
 1304  
 1305  
 1306  
 1307  
 1308  
 1309  
 1310  
 1311  
 1312  
 1313  
 1314  
 1315  
 1316  
 1317  
 1318  
 1319  
 1320  
 1321  
 1322  
 1323  
 1324  
 1325  
 1326  
 1327  
 1328  
 1329  
 1330  
 1331  
 1332  
 1333  
 1334  
 1335  
 1336  
 1337  
 1338  
 1339  
 1340  
 1341  
 1342  
 1343  
 1344  
 1345  
 1346  
 1347  
 1348  
 1349



**Question:** What is the health consciousness index in 2022 based on the chart coordinates?

**Answer:** 12

**CoT Data:** <think>

Step 1: Locate the year "2022" on the x-axis.

Step 2: Identify the data point for the "Health Consciousness Index" line at this year. It is represented by an upward-pointing triangle marker (^) on the dashed red line.

Step 3: Follow the vertical position of this marker upward to the right y-axis, which is labeled "Health Consciousness Index" and ranges from 0 to 80 in increments of 10.

Step 4: The marker aligns exactly with the 78 mark on the right y-axis.

Step 5: Giving the Answer is 78.</think>

<answer>12</answer>

Figure 9: Example 2 of CoT Dataset

1350

1351

1352

1353

1354

1355

1356

1357

1358

1359

1360

1361

1362

1363

1364

1365

1366

1367

1368

1369

1370

1371

1372

1373

1374

1375

1376

1377

1378

1379

1380

1381

1382

1383

1384

1385

1386

1387

1388

1389

1390

1391

1392

1393

1394

1395

1396

1397

1398

1399

1400

1401

1402

1403

## Chain of Thought(CoT) Prompt:

### ROLE

You are an expert vision-language analyst.  
Your job is to look at the image, read the question, and provide a answer.

### CRITICAL RULES (must follow all)

1. **\*\*STEPBYSTEP THINKING:\*\*** You need to think step-by-step first before answering the question. Your thought process (**which you may output in the <think> tag**) should explicitly focus on:
  - \* **\*\*Axes:\*\*** What do the horizontal (X-axis) and vertical (Y-axis) represent? Note their labels, units, and scale.
  - \* **\*\*Data Points:\*\*** Locate the specific bars, points, lines, or other points relevant to the question.
  - \* **\*\*Context:\*\*** Read the chart's title, legend, and any other text to fully understand the context.
2. **\*\*FINAL ANSWER\*\*** Your output MUST contain the answer tag: `<answer>your answer</answer>`.
3. **\*\*STRICT FORMAT:\*\*** The answer inside the `<answer>` tag must be the final, concise result (e.g., a single number). Do not include explanations or units unless required by the chart's notation.

### INPUT FIELDS

Question : {original\_question}

Figure 10: CoT Prompting Reasoning Steps in ChartVRBench Evaluation

1404

1405

1406

1407

1408

1409

1410

1411

1412

1413

1414

1415

1416

1417

1418

1419

1420

1421

1422

1423

1424

1425

1426

1427

1428

1429

1430

1431

1432

1433

1434

1435

1436

1437

1438

1439

1440

1441

1442

1443

1444

1445

1446

1447

1448

1449

1450

1451

1452

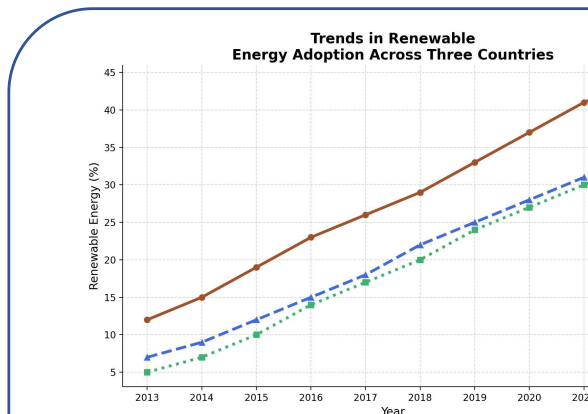
1453

1454

1455

1456

1457



Qwen2.5-VL-7B: CoT Answer

**Reasoning:** To answer this question, I'll follow these steps:

1. Identify the X-axis, which represents the years.
2. Identify the Y-axis, which represents the percentage of renewable energy.
3. Locate the data point for Canada in the year 2020.
4. Read the value on the Y-axis corresponding to that data point.

The data point for Canada in 2020 is located on the green dashed line. **By examining the graph, it appears that the value is just below 28%.**

**Answer:** 28%

CRBench

**Question:** At approximately what renewable energy percentage is Canada shown for the year 2020?

**Answer:** 27

ChartReasoner-7B: CoT Answer

**Reasoning:** The graph shows trends in renewable energy adoption across three countries: Germany, Brazil, and Canada. To determine the renewable energy percentage for Canada in 2020:

1. Locate the year 2020 on the x-axis.
2. Identify the data series for Canada, which is represented by the green dashed line with square markers.
3. Find the point where the Canadian data line intersects the vertical gridline corresponding to 2020.
4. Read the y-axis value at this intersection point.

From the graph, the Canadian data line intersects the 2020 vertical gridline is about from 25 to 30. At approximately 27% on the y-axis.

**Answer:** 27

Figure 11: Example 1 from ChartVRBench comparing the CoT outputs of Qwen2.5-VL-7B and ChartVR-7B.

1458

1459

1460

1461

1462

1463

1464

1465

1466

1467

1468

1469

1470

1471

1472

1473

1474

1475

1476

1477

1478

1479

1480

1481

1482

1483

1484

1485

1486

1487

1488

1489

1490

1491

1492

1493

1494

1495

1496

1497

1498

1499

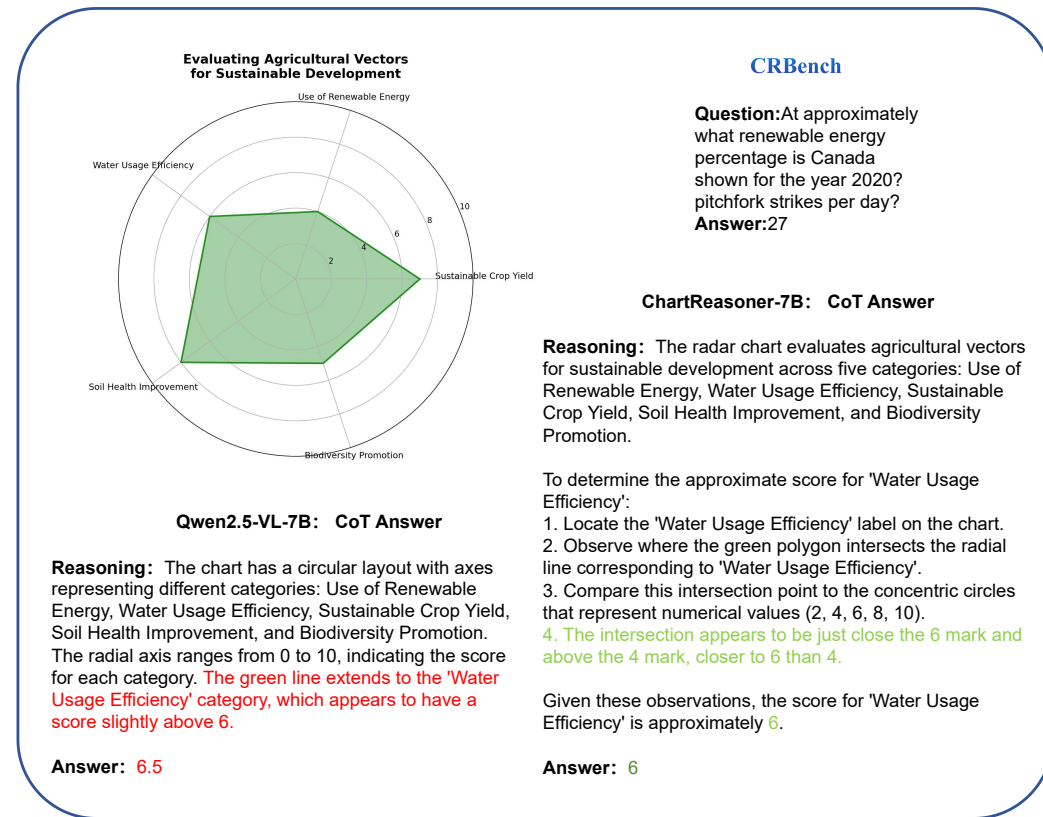


Figure 12: Example 2 from ChartVRBench comparing the CoT outputs of Qwen2.5-VL-7B and ChartVR-7B.

1500

1501

1502

1503

1504

1505

1506

1507

1508

1509

1510

1511